# Computer Aided Structure Based Design of Multitarget Leads for Alzheimer's Disease

José L. Domínguez,[1] Fernando Fernández-Nieto,[2] Marian Castro,[3] Marco Catto,[4] M. Rita Paleo,[1,2] Silvia Porto,[2] F. Javier Sardina,[2] José M. Brea,[3] Angelo Carotti,[4] M. Carmen Villaverde,[1]* and Fredy Sussman[1]*

[1] Departamento de Química Orgánica, Facultad de Química, Universidad de Santiago de Compostela, 15782-Santiago de Compostela, Spain.

[2] Centro Singular de Investigación en Química Biológica y Materiales Moleculares (CIQUS), Universidad de Santiago de Compostela, 15782-Santiago de Compostela, Spain.

[3] Departamento de Farmacología, Instituto de Farmacia Industrial, Centro de Investigación en Medicina Molecular y Enfermedades Crónicas (CIMUS), Universidad de Santiago de Compostela, 15782-Santiago de Compostela, Spain.

[4] Dipartimento di Farmacia-Scienze del Farmaco, Università degli Studi di Bari "Aldo Moro", 70125-Bari, Italy.

**ABSTRACT**

Alzheimer's disease is a neurodegenerative pathology with unmet clinical needs. A highly desirable approach to this syndrome would be to find a single lead that could bind to some or all biomolecules that participate in the amyloid cascade, the most accepted route for Alzheimer disease genesis. In order to circumvent the challenge posed by the sizable differences in the binding sites of the molecular targets we propose a computer assisted protocol based on a pharmacophore and a set of required interactions with the targets, screened by a combination of docking and molecular dynamics protocols. The original scaffold allowed us to identify a set of carbazole containing compounds that initially showed affinity only for the cholinergic targets in our experimental assays. Two cycles of design based on our protocol led to a new set of analogues that were synthesized and assayed. The assay results revealed that the designed inhibitors improve their affinity for BACE-1 by more than three orders of magnitude, as well as displaying amyloid aggregation inhibition and affinity for AChE and BuChE, a result that led us to a group of multitarget amyloid cascade inhibitors that also could have a positive effect at the cholinergic level.

## INTRODUCTION

Alzheimer's disease (AD), a cerebral neurodegenerative pathology that is the main cause of dementia in older people, is characterized by the progressive formation of insoluble amyloid plaques and fibrillary tangles. In spite of the enormous efforts carried out by academic institutions and pharmaceutical industry, AD is an illness with unmet needs since the only drugs available in clinic (i.e., Acetylcholinesterase (AChE) inhibitors and a NMDA receptor antagonist) have a palliative effect and do not modify the course of the disease.[1]

The most accepted hypothesis for the origin of AD is the one related to the amyloid cascade, which singles out the aggregates and fibrils of the amyloid peptide (Aβ, a peptide of 40 or 42 residues) as the cause of AD, since their presence interrupts the synaptic connections and precludes the right inter-neuron orientation.[2,3] The Abeta peptides are produced by the hydrolysis of the amyloid precursor protein (APP) by two aspartic proteases (γ-secretase and BACE-1). The last decade has witnessed an all out effort to discover inhibitors of these two enzymes that could become drug leads for the treatment of AD, but all the candidates have failed either at pre-clinical or clinical stages.[3] The inhibition of Aβ peptide aggregation has become an important target for drug lead discovery in itself, although no Abeta aggregation inhibitor has surpassed the clinical assays either.[1] On the other hand Inestrosa et al.[4] have shown that the peripheral anionic site (PAS) in AChE could be a therapeutic target, since it is a nucleation site for the amyloid Abeta peptide aggregation and hence its inhibition could hinder this process. Finally, the leads that bind AChE, could also bind butirylcholinesterase (BuChE), and hence have a bearing on the cholinergic pathway by precluding the hydrolysis of acetylcholine and probably enhancing (albeit temporarily) cognition in AD patients.

The multiplicity of amyloid cascade AD targets (described above) opens the door to a new approach towards single molecule polypharmacology, which entails the search of a molecule that could bind to all or some targets of the amyloid cascade. This novel paradigm which deviates radically from the one target one molecule strategy has recently received increasing attention.[5-7] Probably the major hurdle in the search for multitarget leads lays on the substantial structural and sequence specificity differences amongst the binding sites of the amyloid cascade targets, which hinders drastically this therapeutic strategy.[6] These differences are especially noticeable between BACE-1 and the other amyloid cascade targets like AChE and Abeta peptides aggregation. It has

been shown that the compounds aimed at these latter targets share some common traits (like the presence of aromatic moieties), an issue that explains the large body of work on this multitarget subset.[7] It would be desirable to find a systematic computer assisted protocol leading to compounds that bind to the largest set of amyloid cascade targets. Herein we postulate the existence of a pharmacophore for multitarget approach to the amyloid cascade of AD, which bears some of the traits of the know leads that bind a variety of amyloid cascade targets.[5-7] This scaffold could be used for systematic search of novel multitarget leads. As a proof of concept, our pharmacophore has enabled us to identify in the literature some candidates bearing the structural requeriments of our proposed scaffold.[8] Nevertheless, the results of our experimental binding assays indicate that although these compounds bind AChE, they have a modest fibril inhibition and display much lower affinities for BACE-1. Our main endeavour in this work was to generate congeneric ligands with better affinities for the all the amyloid cascade targets. For this sake we developed a protocol that relies on molecular docking based screening for the enzyme targets and molecular dynamics simulations for peptide aggregation in order to search for more potent analogues of our starting candidates. The main novelty of the protocol elaborated by us is that it allows for systematic search of multitarget leads and their subsequent optimization, given the fact that our hit docking poses should comply with the set of inhibitor-protein interactions assigned to our pharmacophore. Review of the predicted docking poses in AChE and BACE-1 revealed possible ways of enhancing binding affinity. Two cycles of design based on our protocol lead to a new set of analogues that were synthesized and assayed. The assay results revealed that the designed inhibitors improve their affinity for BACE-1 by more than three orders of magnitude, as well as showing affinity for amyloid aggregates, AChE and BuChE, a result that led us to a group of truly multitarget candidates that interrupt the amyloid cascade while having a positive effect at the cholinergic level.

Furthermore, our results have allowed us to explore some basic questions that relate to molecular recognition issues in the different amyloid cascade targets, including the charge state of the BACE-1 main anchoring group and the way in which the best leads may interrupt the amyloid peptide aggregation.

**Multitarget amyloid cascade pharmacophore**.

Our pharmacophore was built by identifying the specific moieties that are recognized by the binding pockets of the different amyloid cascade targets. For instance, an essential feature in BACE-1 inhibitors is a functional group (such as hydroxyethylene, hydroxyethylamine, guanidium, etc.) which is able to interact through hydrogen bonds and ion pairs with the Asp dyad, the catalytic machinery of this enzyme.[9] Our choice for this kind of functionality has been based on recent studies in our lab that have identified the hydroxyethylamine as an Asp dyad anchor which favours good performance at cellular level.[10,11] On the other hand, an overview of the AChE inhibitors indicate that many of them contain one or two aromatic moieties which interact through π-stacking interactions with clusters of aromatic residues present both in the catalytic anionic site (CAS) and in the peripheral binding site (PAS).[12] Both AChE binding sites are separated by a long gorge. Hence, our ideal AChE inhibitor should include an optimum length spacer that will connect the aromatic moiety residing in the CAS with the one at the PAS. If we accomplish this aim, the resulting lead should have both a palliative effect on AD and hinder amyloid aggregation. Finally, some of the amyloid aggregation inhibitors share with the AChE ligands a common feature, that is, the presence of aromatic groups that target some of the residue clusters rich in aromatic residues present in the amyloid peptide (such as the LVFFA segment). Hence, a multitarget pharmacophore and its possible interactions in the amyloid cascade binding sites could be described by a scheme such as the one presented in Figure 1. A number of the features that appear in this pharmacophore have been used in the search of multitarget cascade leads.[5-7] Herein we demonstrate that the pharmacophore described could be used for multitarget screening and subsequent lead optimization.

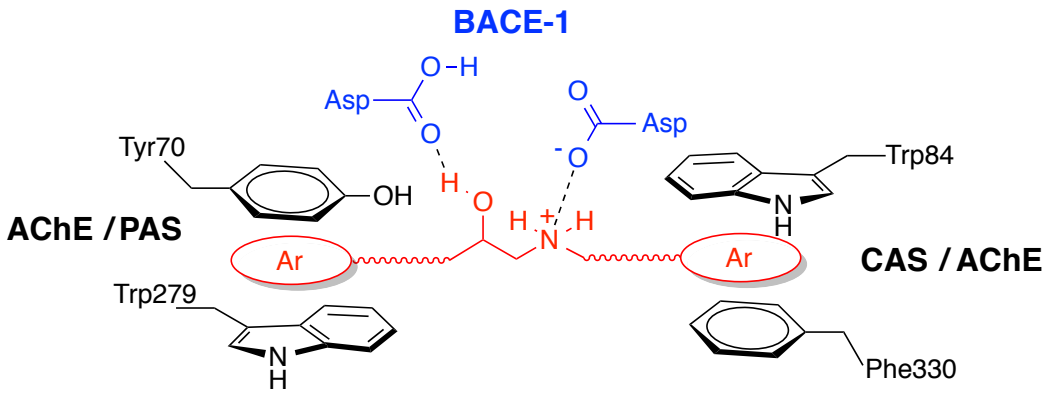


**Figure 1.** Schematic view of our multitarget pharmacophore (red) bound to the Asp dyad of BACE-1 (blue) and to the CAS and PAS of *Tc*AChE (black).

The computer assisted search for candidates based on the pharmacophore shown in Figure 1 lead us to find some compounds (**1**) (see Figure 2) with neurogenerative and neuroprotective properties in mice.[8] Nevertheless, the molecular therapeutic targets for these compounds have not been identified. The stated aim of the study that led to these compounds in the first place was to find analogues of dimebon, a carbazole derivative that in itself showed good promise in AD assays in animals but failed in phase three clinical trials.[13] Moreover, other carbazole derivatives have shown to be good Abeta aggregation inhibitors.[14] As seen from structure **1** in Figure 2, these compounds present all of the structural features that make them good leads for all amyloid cascade targets. On one hand the hydroxyethylamine moiety provides an anchor for BACE-1 binding, while the aromatic moieties on both ends (carbazole and substituted phenyl groups) could be a source of affinity of these compounds for AChE and Aβ peptide oligomers. Based on this information we decided to investigate if the original group of compounds (**1**) owed its beneficial properties at the CNS level to their binding to some of the amyloid cascade targets, and whether we could produce analogues with better affinity for a wider range of amyloid cascade targets.

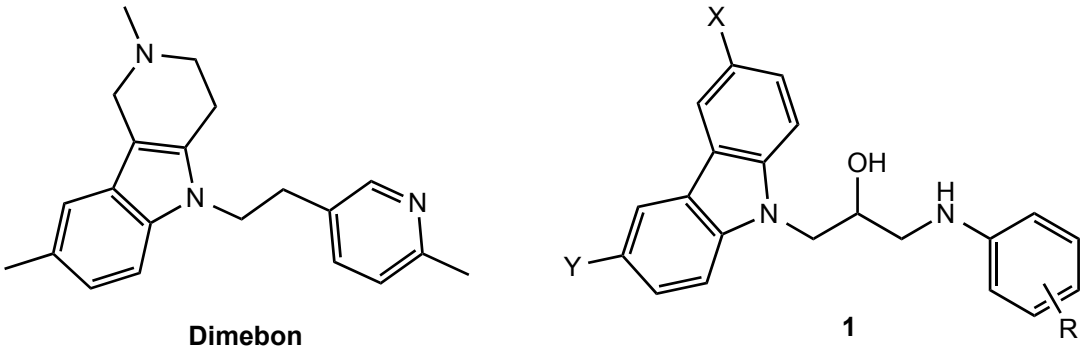


**Figure 2.** Structure of dimebon and its analogues (**1**) studied in this work.

## COMPUTATIONAL METHODS

**Docking protocols.** We carried out the docking simulations with the suite of modules resident in the program GOLD.[15] For each docking run we employed a minimum of 100,000 and a maximum of 1,250,000 genetic generated poses. We scored the poses with three of the scoring functions resident in GOLD (i.e., GoldScore,[16,17] ChemScore[18-20] and ChemPLP[21] ).

**Docking to BACE-1**. One of the most outstanding structural features of the active site of BACE-1 is a residue segment that forms a flap (residues 69 to 75) whose conformational variability allows for a great variety of binding poses for those inhibitors differing in size and shape.[9] This loop, which forms part of the S1 pocket, closes in onto the active site during substrate catalysis. There are inhibitors that bind explicitly to the flap avoiding its closure and hence hampering catalysis. Perusal of the many BACE-1-inhibitor complex structures indicates that the flap presents a wide variety of openings depending on the inhibitor's chemical nature. In order to take into account the flap variability in our docking calculations, we have carried out our docking simulations with three protein templates that differ in the opening of this loop. The first of these protein structures comes from the complex between BACE-1 and the peptide-mimetic inhibitor **OM99-2** (PDB entry 1FKN) and has a closed flap.[22] The second structure has a non-peptidic inhibitor bound to the enzyme with a middle range opening of the flap (PDB entry 3KMY),[23] while the last template was obtained from the unbound structure of BACE-1, and has a fully opened flap (PDB entry 1W50).[24] Figure 3 exhibits the superposition of these three structures with the flap structures displayed in different colors.

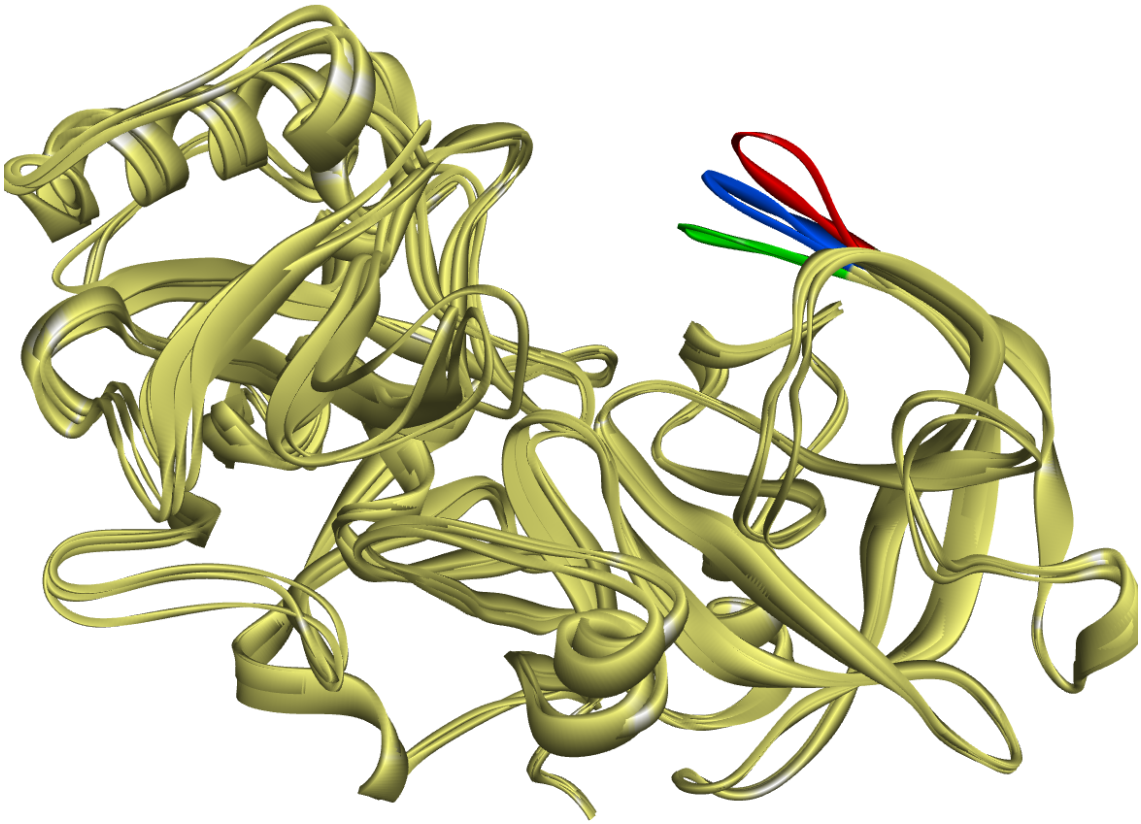

**Figure 3.** Superimposition of 1FKN, 3KMY and 1W50 protein ribbon structures. The flap loops are colored in green, blue and red respectively.

Our previous studies, which combined SPR binding experiments with molecular mechanics based calculations, predicted that the Asp dyad in BACE-1 has a monoprotonated state (at pH values ranging from 4.5 to 7.4) when bound to compounds with a hydroxyethylamine moiety.[10] Thus, we assigned this Asp dyad state to BACE-1 in our BACE-1 docking screening calculations. On the other hand, the aniline present in our compounds could be protonated or neutral at the acidic pH (4.5-5.0) at which the experimental assays are carried out. For this reason docking simulations for these compounds were carried out both with neutral and protonated anilines.

As a first step we cleaned up the target structures mentioned above, eliminating the crystallographic water molecules, discarding alternative conformations and adding hydrogen atoms, by using the Discovery Studio (DS) modules.[25] We defined the targeted binding site for GOLD docking to these proteins as all the atom residues that were within 6Å of the inhibitor in the 3KMY complex.

For each of the structures differing in the flap opening, we then performed docking calculations with one of the three scoring functions (ChemScore, GoldSCore and ChemPLP). In each of the runs we searched for the presence of a single hit pose amongst the top ten docking resulting poses. We define a hit pose as the one that will fulfill the hydrogen bond pattern between the hydroxyethylamine fragment and the Asp dyad shown for our pharmacophore in Figure 1. Global success rates for every compound candidate were calculated by adding up the number of single hits of the docking simulations carried out with the three scoring functions for our three protein templates differing in the flap opening described above.

**Docking to AChE**. For the docking predictions to this target we used the X-ray structure of *Torpedo californica* (*Tc*AChE) complexed with a bis-tacrine analogue (PDB entry 1ODC).[26] A close up of the binding pose is shown in Figure 4.

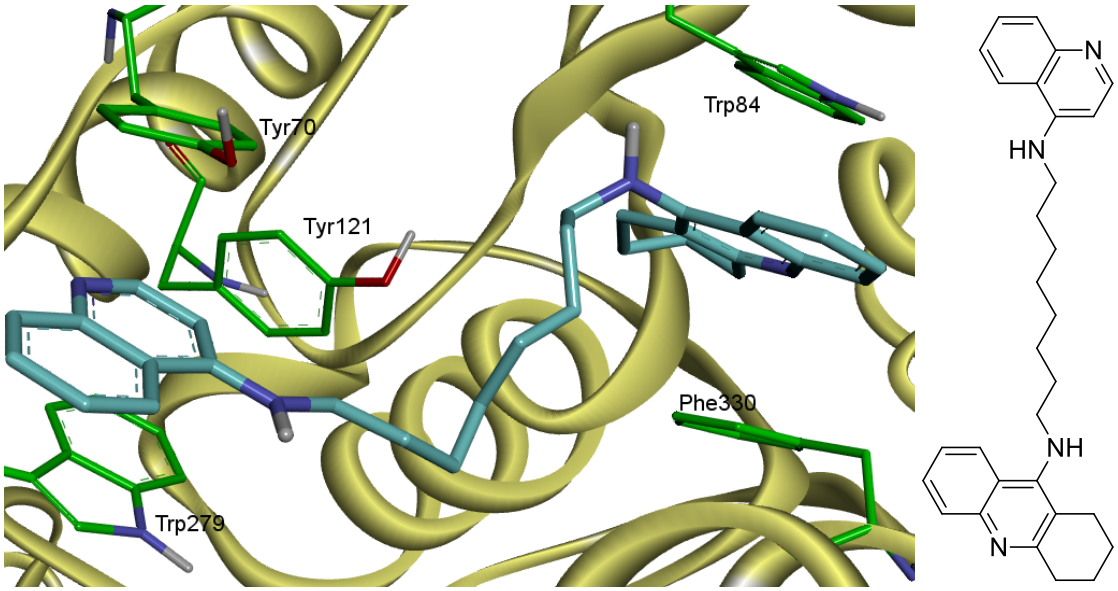


**Figure 4.** Close up to the binding of the bis-tacrine analogue indicated to both binding sites (CAS and PAS) in *Tc*AChE (from PDB entry 1ODC). The inhibitor is shown in blue and the aromatic residues in green. Notice the π-π interactions between the aromatic moieties and the side chains of residues Trp 84 and Phe 330 at the CAS and with residues Tyr 70 and Trp 279 at the PAS.

In the same way as for BACE-1, we cleaned up the target structure (PDB id 1ODC), eliminating the crystallographic water molecules, discarding alternative conformations and adding hydrogen atoms, by using the Discovery Studio (DS) modules.[25] We defined the binding site as all the AChE atom residues that lay at 6 Å from the ligand of this complex (i.e., the bis-tacrine analogue). Again, the docking conformations generated by the genetic algorithm were evaluated by the same scoring functions used for BACE-1. In each run the top ten poses were screened for compliance with the face-to-face π-stacking interactions that will optimize the inhibitor affinity both at the CAS and PAS in AChE, as shown in Figure 1 and exemplified by the bis-tacrine analogue in Figure 4. In the same way as in BACE-1 the hit success rate was determined by searching for a hit amongst the top ten poses for the docking simulations evaluated with our three scoring functions. Global success rates were calculated by adding up the number of single hits.

**Aβ aggregation inhibition protocol**. As we explained in the introduction, one of the therapeutic targets is the inhibition of the Aβ peptide oligomerization that leads to the neuronal toxic species. These peptides do not have a unique binding site for the ligands as in the case of other AD amyloid cascade enzymatic targets. Depending on the nature of the ligand, there are multiple binding sites that share similar sequence motifs. For instance, some aromatic moiety inhibitors tend to bind to aromatic residue clusters

present in the LVFFA segment of the amyloid peptide.[27] Hence, many *in silico* aggregation inhibition studies merge docking protocols with molecular dynamics (MD) simulations.[28] We have explored a different approach recently developed by the group of Caflisch.[27a] It consists in analyzing lengthy MD simulations of a segment of the Aβ peptide (Aβ12-28) in the presence of a given candidate. This peptide fragment has been chosen for several reasons. Firstly, the first 11 residues were omitted since they lack any definite secondary structure in some NMR amyloid aggregate structures.[29] Moreover, the selected segment contains one of the regions (LVFFA) around which a beta hairpin, the template for Abeta aggregation forms, and is also one of the ligand's binding spots for a number of ligands.[27] Finally, this segment has been used in NMR based experiments to study ligand binding locations.[27b]

Our extensive MD calculations were carried out with the CHARMM PARAM-19 force field,[30] which employs an extended atom approximation for all carbon atoms. Protonation states of all titratable residues were considered at neutral pH. In particular the side chains of the His residues were assigned a neutral charge, whereas the basic residues (Arg/Lys) and the acidic residues (Asp/Glu) were assigned either a positive or a negative charge respectively. We used an implicit solvation protocol called FACTS (Fast Analytical Continuum Treatment of Solvent), an efficient generalized Born (GB) implicit solvation model developed in Caflisch's group,[31] which includes a solvent accessible surface of the solute for the non-polar contribution.

MD Simulations were carried out with periodic boundary conditions at a fixed peptide concentration of 2.5 mM (87 Å cubic simulation box) using the Langevin integrator at low friction (coefficient of 0.15 $ps^{-1}$) and at a temperature of 300 K. Using a time step of 2 fs, for each system, we performed five independent runs which added up to a 5 μs trajectory. Each of the starting structures contained the peptide in an extended conformation together with the inhibitor candidate in a different position. We also used as a reference the simulations of a peptide with the known aggregation inhibitor 9,10-anthraquinone and the ligand-free peptide. The initial structures were subjected to two energy minimization runs, which began by a 500 steps steepest descent run followed by a 50,000 steps conjugate gradient calculation. In each case the gradient tolerance was of 0.001 kcal/(mol·$Å^2$). Then, heating stage and a thermal MD equilibration stages spanning 0.5 ns each were carried out, followed by the production stage described above.

Since every MD simulation takes a month wall clock computer time we had to select the kind and number of compounds used in our calculations. For instance, for the indole derivatives we performed simulations only on one aniline and two benzylamine containing compounds (see below). Our simulations were then used to calculate the average residency time of the ligand around the peptide and around every residue of the peptide, as well as the effect of the ligand on the secondary structure of the peptide. The statistical significance of these results is provided by the standard deviations based on the individual trajectories.

## RESULTS

### 1. First lead optimization: Carbazole derivatives.

### 1.1. BACE-1 ligand screening

The first set of compounds studied were the carbazole derivatives bearing an aniline moiety with a substituent either in *ortho* or *meta* positions, that originally showed neuro-protective and neuro-generative activity in mice.[8] From this study we chose a subset whose chemical structures and docking results data are displayed in Table S1 in the supporting info, while the global docking success rates (see methods section for details) are shown in Figure 5. As seen from Figure 5 and Table S1, the compounds that have a methoxy substituent at the aniline either in the *ortho* (compound **1d**) and at the meta position (compound **1g**) are the ones that show the widest consensus as a possible BACE-1 inhibitor. The better fit displayed by these compounds could be the result of reduced steric clashes, given that they are the smallest candidates in this list. For the same reason, our predictions indicate that the smaller ligands bind to BACE-1 with any of the three flap openings (see Table S1). Nevertheless, given their size, it is doubtful that these ligands could span both the CAS and PAS in AChE, and hence become multitarget leads

Perusal of the results in Figure 5 and Table S1 shows that the available hits are obtained almost exclusively when the docking calculations are carried out with a charged ligand. Actually, only two of the seven compounds (**1e, 1g**) display some hits when neutral. This result is in line with our previous studies,[32] which indicate that there is an enrichment in the number of predicted poses close to those observed experimentally when the ligand is charged.

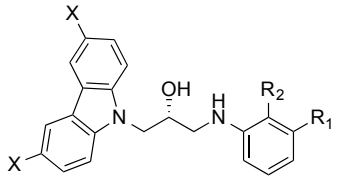


**1a**: X = H, $R_1$ = H, $R_2$ = OMe
**1b**: X = H, $R_1$ = H, $R_2$ = OBn
**1c**: X = H, $R_1$ = H, $R_2$ = $OCH_2CH_2Ph$
**1d**: X = Br, $R_1$ = H, $R_2$ = OMe
**1e**: X = Br, $R_1$ = H, $R_2$ = OBn
**1f**: X = Br, $R_1$ = H, $R_2$ = $OCH_2CH_2Ph$
**1g**: X = Br, $R_1$ = OMe, $R_2$ = H

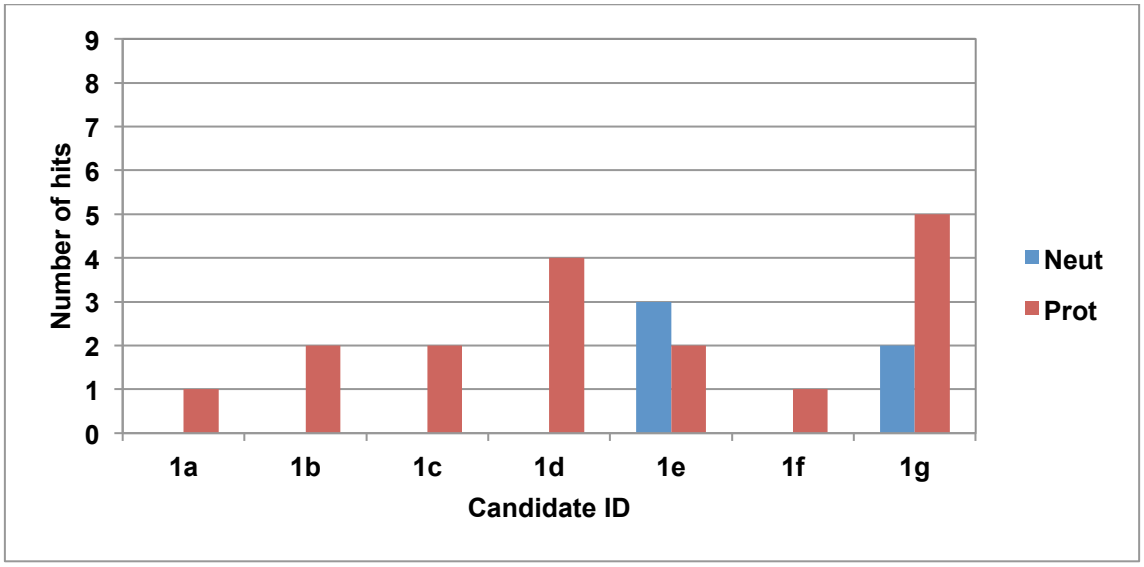


**Figure 5.** Global docking success rates for BACE-1 as provided by the number of single hits across flap openings and docking scoring functions. Neut and Prot indicate weather the ligand is neutral or protonated.

The p$K_a$ of the protonated amino group belonging to the aniline moiety, for these compounds in solution, is ca. 4.7, a value that is close to the pH at which the binding assays are performed. Replacing the aniline by a benzylamine moiety would likely increase the p$K_a$ value of the amino group and hence the likelihood of being charged, an outcome that probably will boost the number of predicted BACE-1 binders. Figure 6 displays the global hit success for benzylamine containing compounds substituted in *ortho* (upper panel) and *meta* (lower panel). The detailed data for these docking calculations are shown in Tables S2 and S3. Comparison of the number of single hits amongst the top ten exit poses between analogous aniline (Table S1 and Figure 5) and benzylamine compounds (Tables S2/S3 and Figure 6), indicates a substantial hit rate increase for benzylamines above those calculated for the aniline containing compounds, an outcome that validates our design premises.

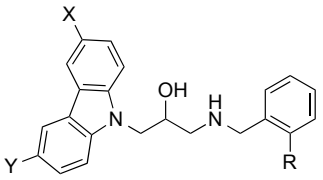


**2a**: X = Y = H, R = OMe
**2b**: X = Y = H, R = OBn
**2c**: X = Y = H, R = $OCH_2CH_2Ph$
**2d**: X = Y = Br, R = OMe
**2e**: X = Y = Br, R = OBn
**2f**: X = Y = Br, R = $OCH_2CH_2Ph$
**2g**: X = Br, Y = Me, R = OBn
**2h**: X = Br, Y = Me, R = $OCH_2CH_2Ph$

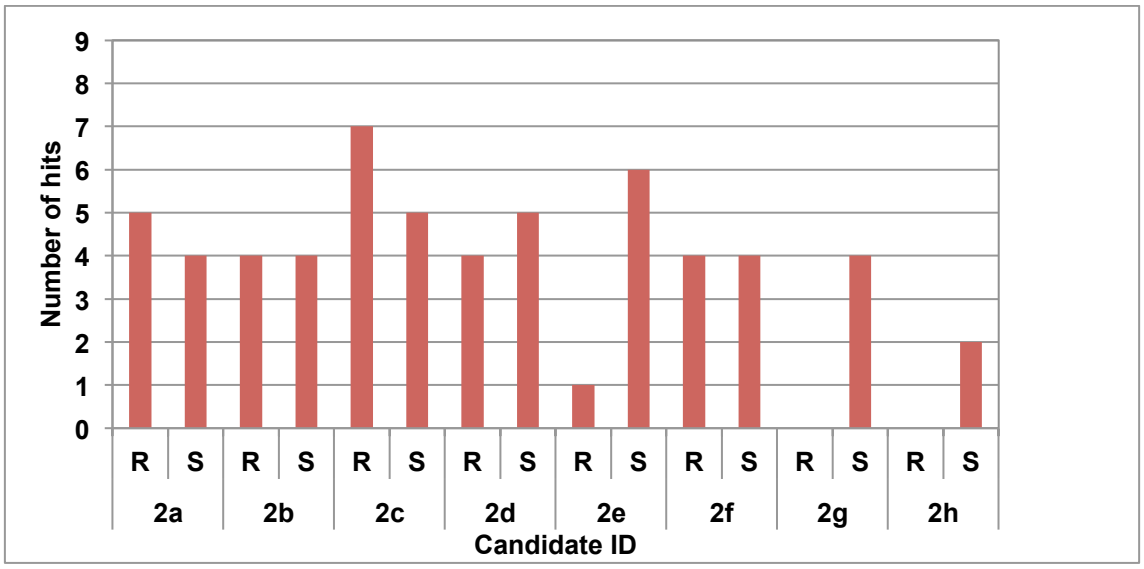


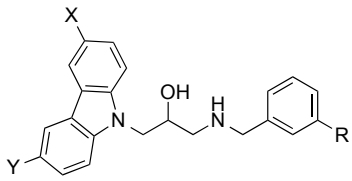


**3a**: X = Y = H, R = OMe
**3b**: X = Y = H, R = OBn
**3c**: X = Y = H, R = $OCH_2CH_2Ph$
**3d**: X = Y = Br, R = OMe
**3e**: X = Y = Br, R = OBn
**3f**: X = Y = Br, R = $OCH_2CH_2Ph$
**3g**: X = Br, Y = Me, R = OBn
**3h**: X = Br, Y = Me, R = $OCH_2CH_2Ph$

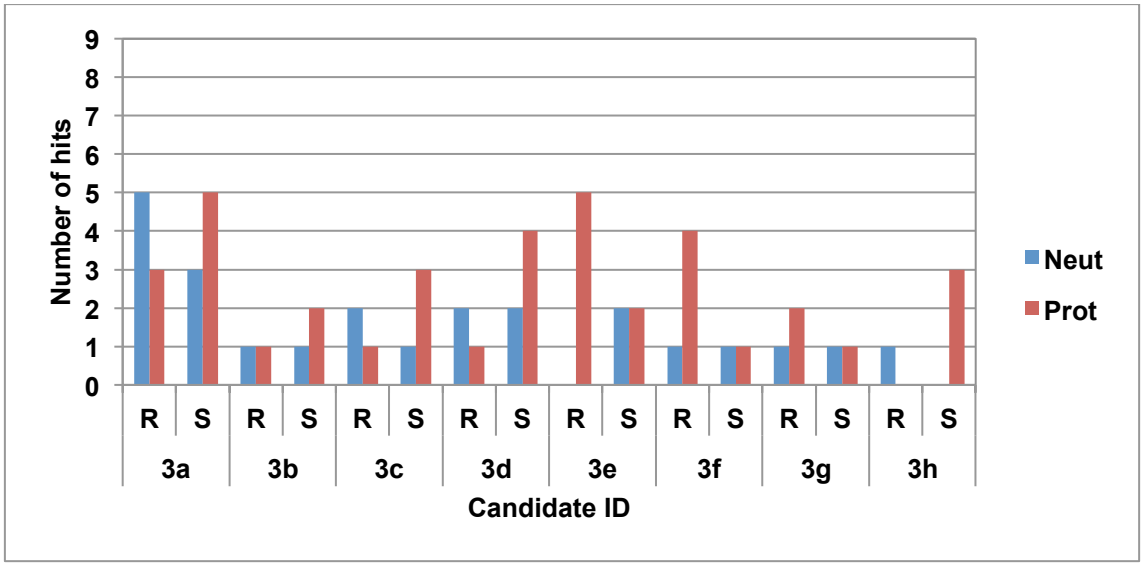


**Figure 6.** Global hit success that result from the docking to BACE-1 of protonated *ortho* (upper panel) and both neutral and protonated *meta* benzylamines (lower panel). R and S indicate the two possible enantiomeric configurations of these compounds.

Perusal of Figure 6 indicates that the benzylamine substitution pattern has also a bearing in the number of possible hits. The results would seem to indicate that the *ortho* is favoured over the *meta* substitution at the benzylamine moiety. For instance amongst the top ten poses, the number single hits with *ortho* substitution is twice the number of hits with the *meta* substitution (see Tables S2 and S3). Nevertheless, there seems to be exceptions (e.g., see compounds **3e** when the hydroxyl group is in the *R* configuration), which had a number of hits comparable to the analogous *ortho* derivative (i.e., compound **2e** when the hydroxyl group is in the *S* configuration).

For the compounds bearing a benzylamine fragment we also analyzed the effectiveness of each stereoisomer. The results shown in Figure 6 do not show a clear predilection for a given enantiomer, as changes at the end points of the candidate compounds seem to change the preference. For instance in the case of the compounds containing *meta*-benzylamines, those compounds that bear two Br atoms on the carbazole favour a *R* configuration (compounds **3e** and **3f**), while those that replace both Br atoms by H atoms favour a *S* configuration. Nevertheless, these configuration patterns do not seem to hold for the *ortho*-benzylamine bearing compounds.

**1.2. AChE ligand screening**

Figure 7 displays the global hit rate for protonated anilines and benzylamines (substituted in the *ortho* position), while Figure 8 depicts the number of hits for the compounds bearing benzylamines substituted in *meta*. As seen from these figures, there is a wide consensus amongst the scoring function results, indicating that these compounds are good candidates for AChE inhibitors, in most cases independently of the stereochemistry of the hydroxyl group and the charge of the hydroxylethylamino group. Comparison with the BACE-1 docking results described above indicates that the number of predicted hits for AChE is substantially larger than those for BACE-1, implying that there are fewer hurdles for finding a candidate that will fulfil the pharmacophore requirements for the former enzyme.

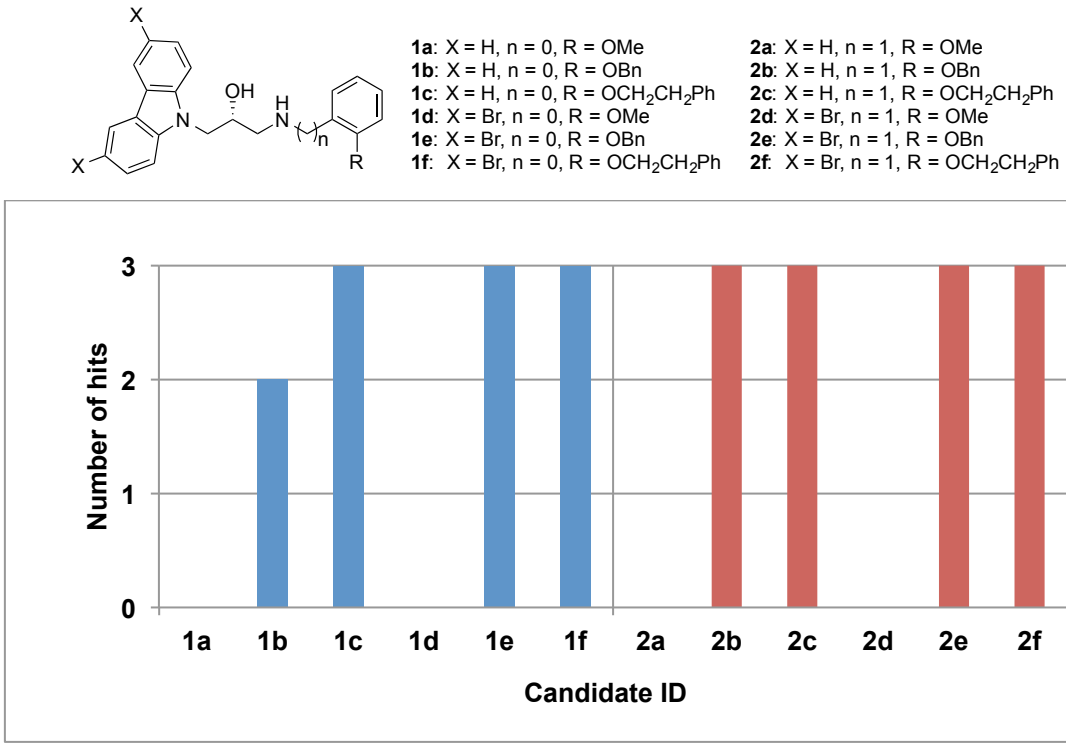


**Figure 7.** Global hit rate resulting from the AChE docking screening of the protonated *ortho* substituted anilines (left) and benzylamines (right). The hit search was carried amongst the top ten poses resulting from three docking calculations each carried out with a different scoring function (ChemScore, GoldScore and ChemPLP).

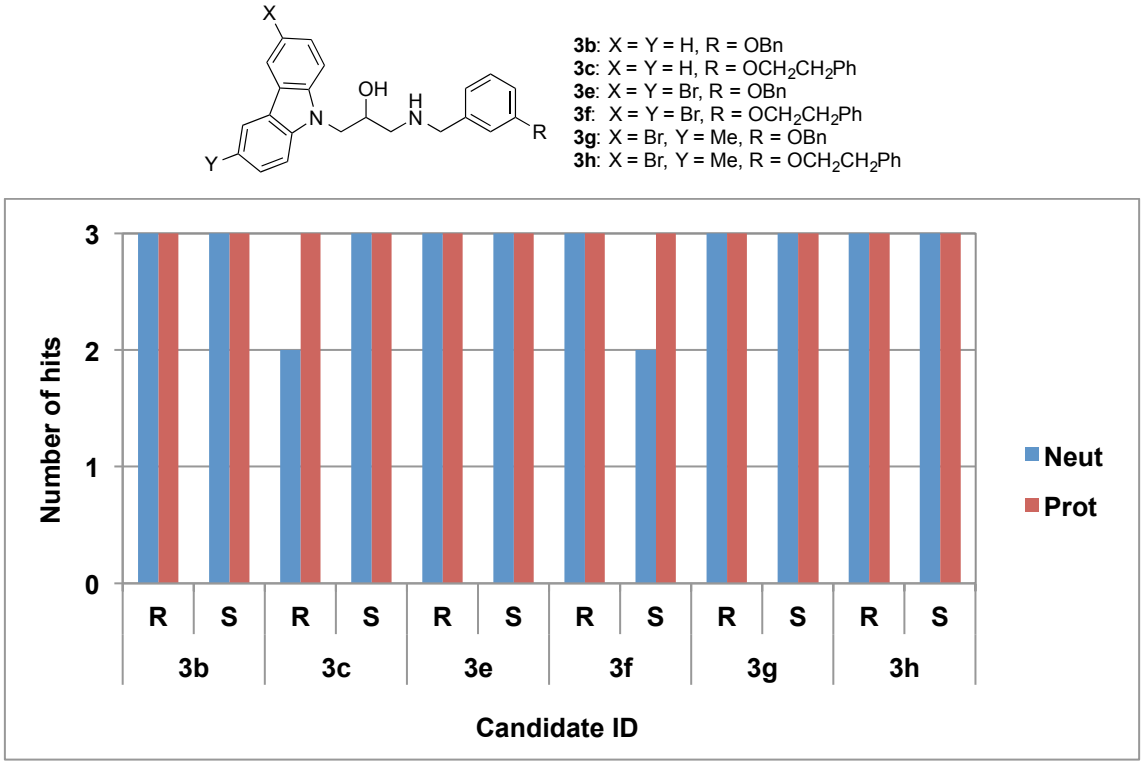


**Figure 8.** Global hit rate resulting from the AChE docking screening of the compounds with a *meta* substituted benzylamine. For each molecule we studied the effect of the stereochemistry of the hydroxyl group (*R*, *S*) and the protonation state of the amine group.The hit search was carried amongst the top ten poses resulting from three docking calculations each carried out with a different scoring function (ChemScore, GoldScore and ChemPLP).

The scoring function values for aniline and benzylamine containing compounds are listed in Tables S4 and S5. Perusal of Table S4 and Figure 7 indicates that the shorter compounds, like **1a**, **1d**, **2a** and **2d** (those bearing a methoxy substituent) have no hit according to our pharmacophore definition, as shown in Figure 1. Scrutiny of the binding poses for a methoxy as compared to a benzyloxy substituted compound (Figure 9) indicates that the former ligands derive their worse performance from their inability to bind both to the CAS and PAS in AChE. As seen from Figure 9 the carbazole moiety interacts in the CAS with residues Tyr 84 and Phe 330 through π stacking interactions. The shorter ligand is not able to reach the PAS in AChE and hence to generate these types of interactions with Tyr 70 and Trp 279.

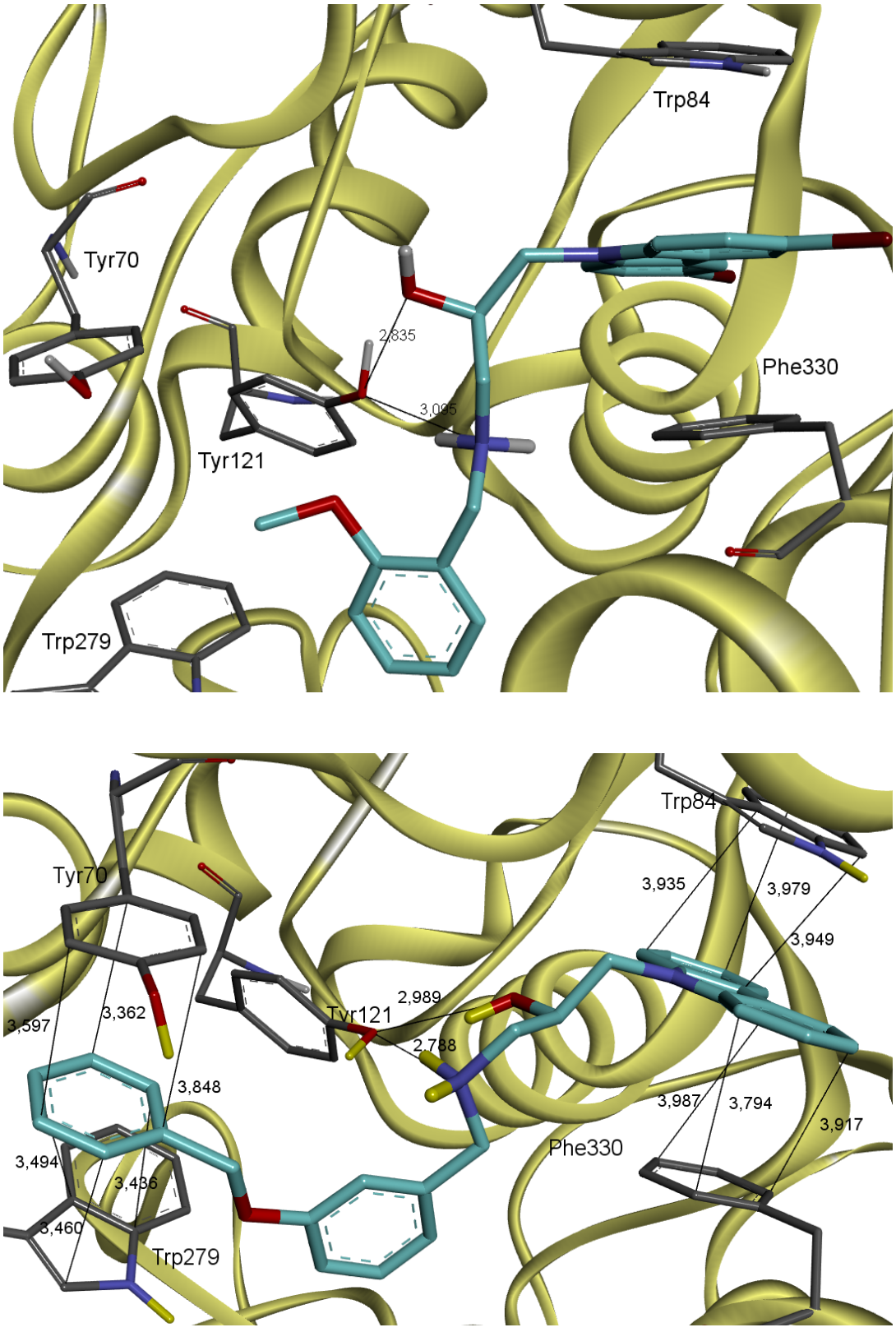


**Figure 9.** Docking of compounds **2d** (upper panel) and **3b** (lower panel) into AChE.

### 1.3. Inhibitor Aβ12-28 peptide interaction results.

Table 1 lists the fraction residence times for 9,10-anthraquinone (a reference compound) and for some carbazole containing compounds, up to 7.5 Å from the peptide. We have also calculated the residence time of these ligands around every residue of the peptide with a cut-off distance of 4.5 Å (see Figure 10) and the residue-residue interaction in the absence and presence of the ligands (see Figure 11 and S4). As seen from Table 1, the candidate compounds have a much larger residence time than the reference ligand. Moreover, the selected compounds display a bigger preference (than the reference compound) for the binding hot spots centered on both the His cluster at the N terminal end and on the aromatic cluster found at the LVFFA segment.

**Table 1.** Fraction residence time for contacts peptide-ligand up to 7.5 Å.

| Candidate | Contact Time |
|---|---|
| 1b | 0.93 |
| 1c | 0.90 |
| 1d | 0.99 |
| 1f | 0.99 |
| anthraquinone | 0.36 |

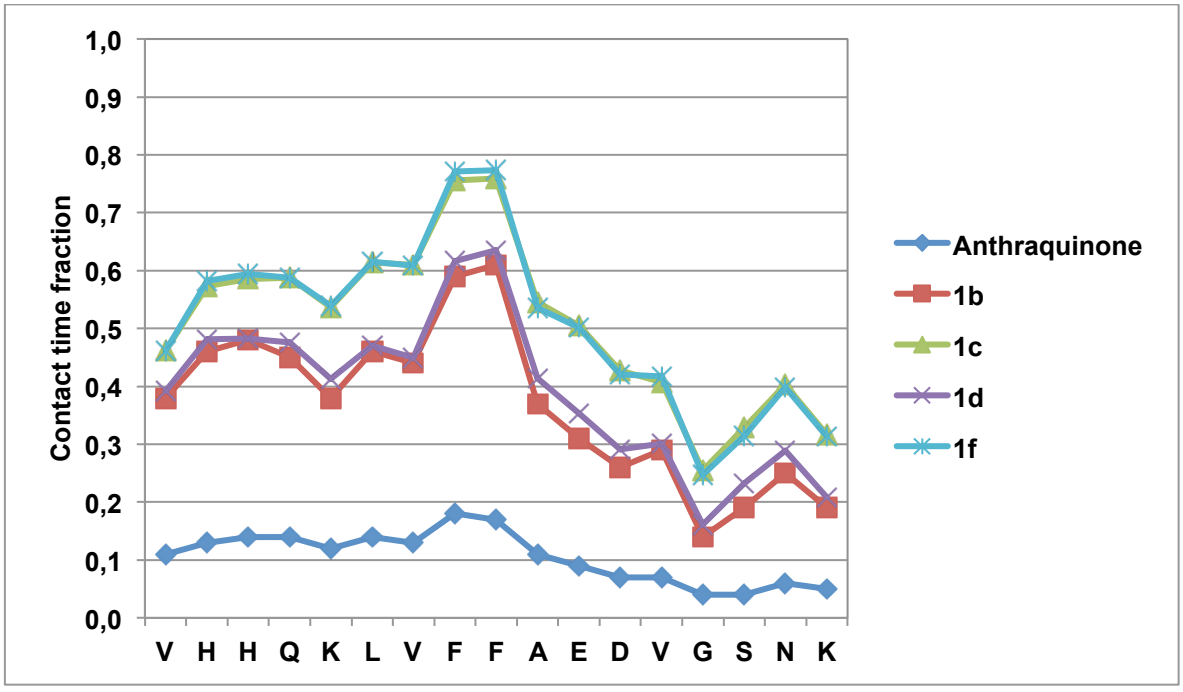


**Figure 10.** Ligand-peptide residues fraction contact times. Cut-off distance is set at 4.5 Å.

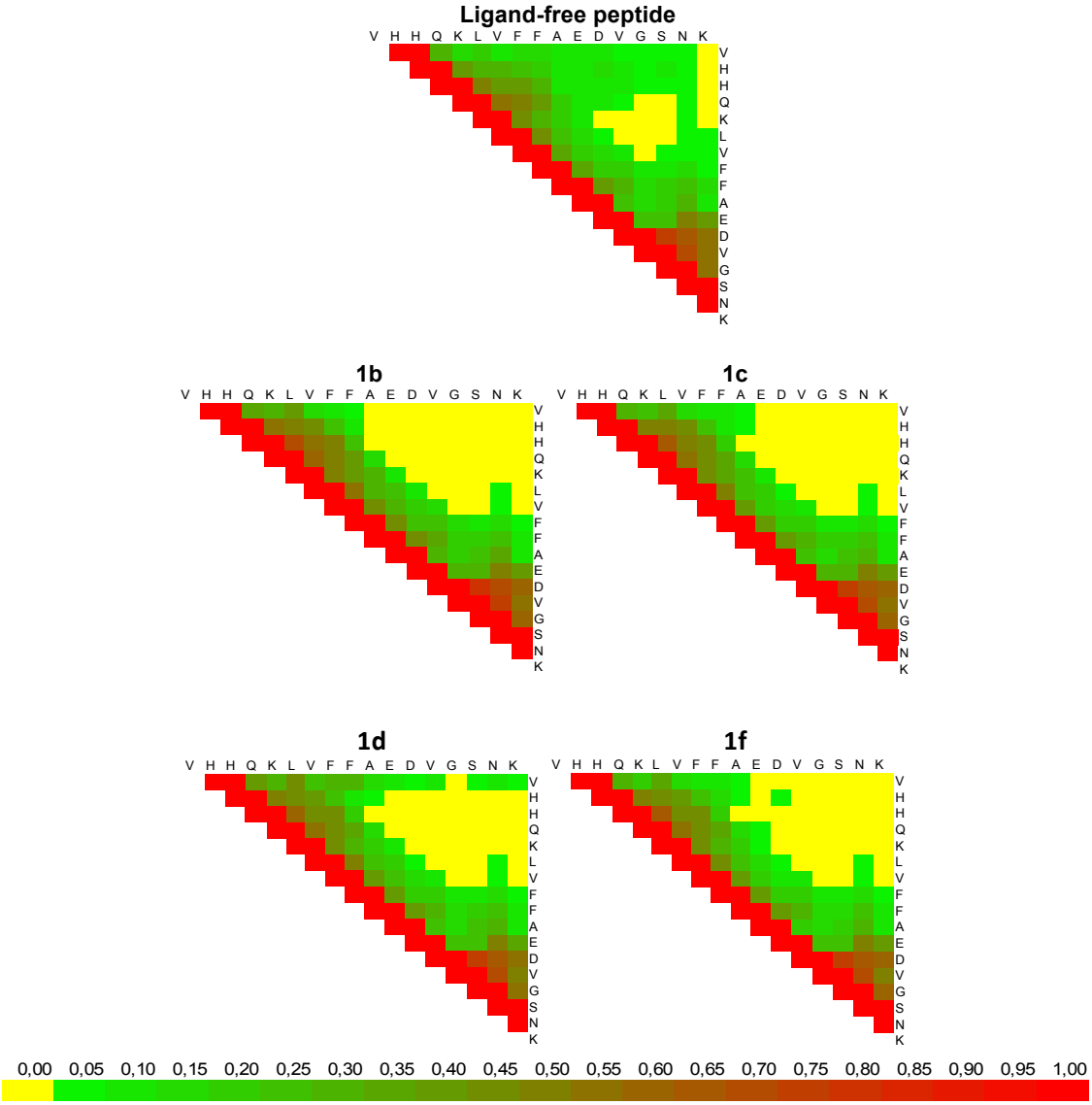


**Figure 11.** Residue-residue contact map in the absence (top panel) and in the presence of inhibitors. The colour scale shown above indicates the fraction residence times.

An important issue is the effect of the ligand on the secondary structure of the peptide. The Aβ peptide, which originates from APP hydrolysis, originally adopts a helix structure. As amyloid aggregates are formed, there is a change of conformation that leads to a beta hairpin, specifically around the DVGS motif. For instance the NMR structure of a pentamer[29] shows clearly that the peptides organize themselves forming hairpins that aggregate as sheets. As seen from Figure 11 and S4, the ligands would seem to partially preclude the formation of this secondary structure motif (turn) in a monomer, a process that may lead to reduced aggregation. Hence, it may be surmised that the residue-residue contact map in the presence of a ligand may give us a measure of the inhibitory aggregation effect of our candidates.

**1.4. Synthesis and experimental assays for carbazole containing compounds**.

The synthesis of several carbazole-containing compounds was carried out following Scheme 1, which includes the list of synthesized molecules. Carbazole-epoxide **10** was prepared as described in the literature from carbazole (**8**) and epichlorohydrin **9**.[8,33] Regioselective ring-opening of epoxide **10** with different *ortho*-substituted anilines **11** in the presence of $Mg(ClO_4)_2$ in acetonitrile,[34] afforded carbazole compounds **1** in moderate to good yields. Similarly, as shown in Scheme 1, carbazole analogues **3** were synthesized by ring-opening of carbazole-epoxide **10** with *meta*-substituted benzylamines **12**. The choice of compounds was guided in many cases by the availability of the reactants. Although in the case of benzylamines the compounds with an *ortho* substituent seem to show a wider consensus as BACE-1 inhibitors across all scoring functions (see Figure 6), they require a more elaborated and expensive chemistry. For this reason, we chose the best scoring candidates with a *meta* substituted benzylamine (**3e** and **3f**).

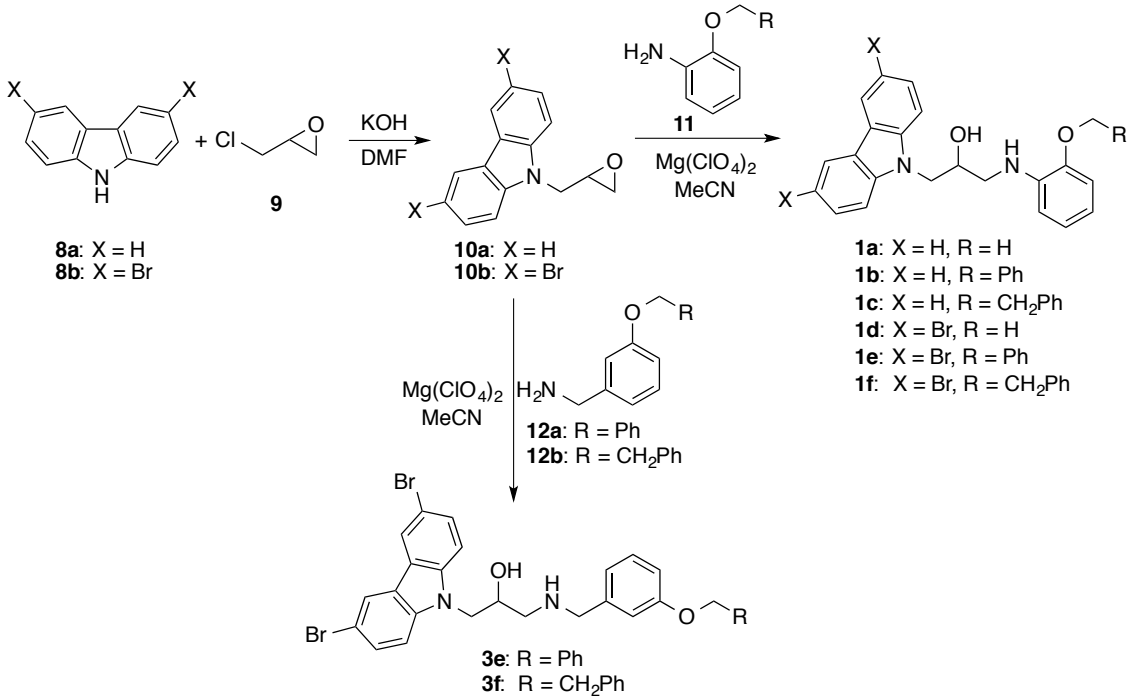


**Scheme 1.** Synthetic route and carbazole derivatives synthesized.

The results for the experimental binding assays in BACE-1, AChE and BuChE, as well as the ThT Aβ aggregation inhibition are shown in Table 2. As seen from this table, some of the aniline-containing compounds showed some promise as multitarget

inhibitors. For instance, compounds **1e** and **1f** display μM affinity for AChE and Aβ inhibition percentage of ca. 50% at 100 μM peptide concentration, values that are superior to 9,10-anthraquinone (30% at 100 μM).[35] On the other side compound **1a**, displays μM binding for BuChE, and 58% percentage of inhibition of the fibril formation. Nevertheless, none of the carbazole and aniline containing compounds, which were originally shown to be neuroprotective and neurogenerative in mice,[8] resulted in multitarget leads across all the chosen amyloid cascade targets.

**Table 2**. Experimental results for the multitarget assays.

| Compound | *Ee*AChE | | hsBuChE | | Aβ(1-40) | BACE-1 | |
|---|---|---|---|---|---|---|---|
| | %Inh.@ 10μM | $IC_{50}$(μM) | %Inh.@ 10μM | $IC_{50}$(μM) | %Inh.@ 100μM | %Inh. @100μM | $IC_{50}$(μM) |
| **1a** | 30 ± 1 | -- | -- | 6.0 ± 1.0 | 58 ± 2 | 1.3 ± 0.3 | -- |
| **1b** | 22 ± 1 | -- | 34 ± 1 | -- | 51 ± 5 | 2.4 ± 1.4 | -- |
| **1c** | 49 ± 2 | -- | 33 ± 1 | -- | 36 ± 5 | 1.5 ± 0.3 | -- |
| **1d** | 15 ± 1 | -- | 12 ± 1 | -- | 41 ± 3 | 1.6 ± 1.5 | -- |
| **1e** | -- | 7.2 ± 0.4 | 20 ± 1 | -- | 46 ± 3 | 0.5 ± 0.3 | -- |
| **1f** | -- | 7.8 ± 0.2 | 10 ± 1 | -- | 49 ± 1 | 0.9 ± 0.9 | -- |
| **3e** | 48 ± 1 | -- | -- | 1.1 ± 0.2 | 11 ± 3 | -- | 3.1 ± 0.4 |
| **3f** | -- | 14 ± 1 | -- | 7.1 ± 0.7 | 28 ± 3 | -- | 3.1 ± 0.3 |

Finally, as seen from this table the benzylamine amine bearing compounds (**3e** and **3f**) have improved their affinity for BACE-1 by three orders of magnitude over the aniline containing compounds. This result validates and supports the outcome of our calculations (see Figures 5 and 6), which indicate that the addition of a $CH_2$ fragment provides hits across the set of scoring functions used in our calculations. As mentioned before this effect is probably due to the raise in the p*K*a in the benzylamine's amino group, which favours the formation of an ion pair with one of the Asp residues of the active site Asp dyad. These latter compounds (**3e** and **3f**) have improved their affinity for BuChE and **3f** displays as well a micromolar affinity for AChE. Nevertheless, their Abeta aggregation inhibition has dropped below the 30% inhibition displayed by the reference compound (9,10-anthraquinone).

**2. Screening a third generation candidates: Indole based multitarget candidates.**

The carbazole moiety present in the candidates synthesized and assayed above is quite a bulky group. Perusal of the resulting binding poses showed some steric clashes between the ligand and some protein side chains. The close van der Waals contacts are allowed by the GOLD docking protocol as a way of compensating for the lack of protein flexibility.[15] Figures S1 and S2 display the steric clashes of some ligands with BACE-1

and AChE. An option to avoid the steric clashes altogether will be to search for smaller aromatic groups in place of the carbazole, like an indole. Based on this idea we designed a new generation of multi-target candidates bearing this fragment in one end and in the other end the same aromatic moieties which were already used in the previous sections (substituted anilines and benzylamines). For these ligands we have chosen the OBn substituent for the anilines and benzylamines, since the analysis of the results for the carbazole-containing compounds described above has shown that this substituent provides the leads with the right length to span the distance from the CAS to the PAS in AChE.

**2.1. BACE-1 ligand screening**

Figure 12 lists the global hit success for the indole based derivatives, while the scoring function values for this set of compounds are listed in Tables S6 and S7. The structural variables analyzed in these figures are the same as in the study of the carbazole derivatives in the previous section and include the moiety to which the amino group belongs (aniline or benzylamine), its protonation state, the substitution of the indole group, the substituent position (*ortho* or *meta*) of the other aromatic ring and the stereochemistry of the OH group.

Perusal of our results indicates that the indole based ligands have a higher probability of binding to BACE-1 with a medium open or fully open flap (see Tables S6 and S7). The number of hits with a closed flap is very small, especially when using a ChemPLP scoring function, indicating that these molecules fit in the active site of BACE-1 thanks to the plasticity of its flap.

In the case of the carbazole based compounds, the best ranking compounds where those that contained a benzylamine moiety, one that assured the existence of a protonated amino group. A global comparison of the compounds that contain an aniline (see Figure 12, upper panel) with those that contain a benzylamine (Figure 12, lower panel) indicate that the latter present a larger global hit rate, a pattern similar to that observed for the carbazole containing compounds. Nevertheless, the preferred benzylamine substitution pattern in the indole based compounds (predicted by our calculations) differs from the one predicted for the carbazole containing ligands, since these latter compounds favour an *ortho* rather than *meta* substitution pattern for benzylamines. On the other hand perusal of Figure 12 suggests that the indole based compounds favours a *meta* over the

*ortho* substitution, a substitution pattern also followed by the aniline bearing compounds.

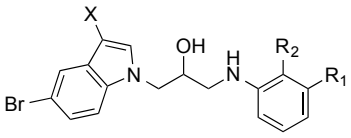


**4a**: $R_1$ = H, $R_2$ = OBn, X = H
**4b**: $R_1$ = H, $R_2$ = OBn, X =Br
**4c**: $R_1$ = H, $R_2$ = OBn, X = Me
**5a**: $R_1$ = OBn, $R_2$ = H, X = H
**5b**: $R_1$ = OBn, $R_2$ = H, X =Br
**5c**: $R_1$ = OBn, $R_2$ = H, X = Me

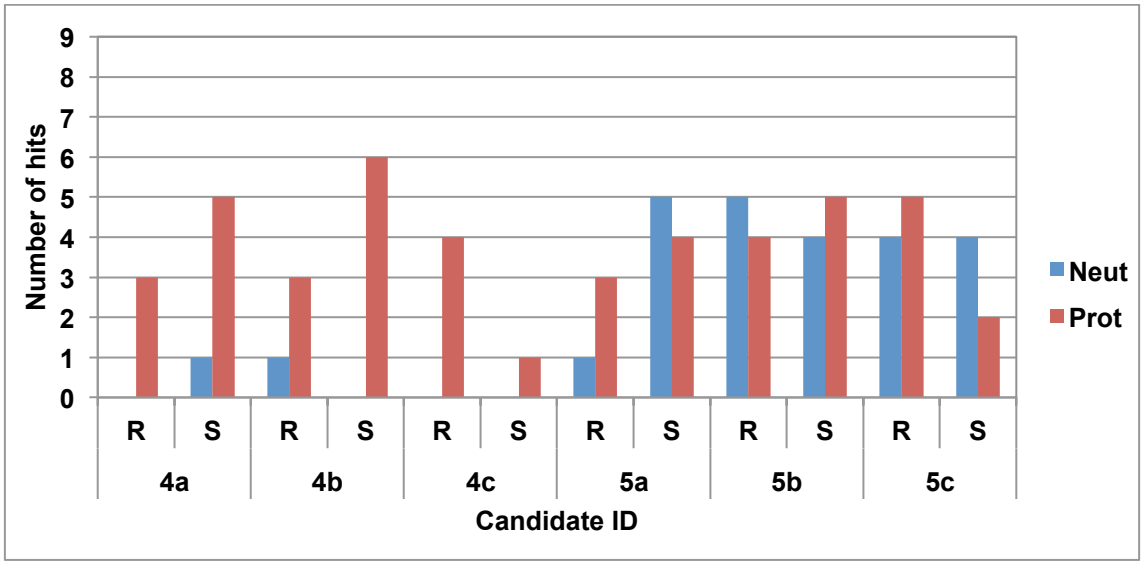


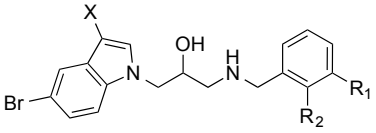


**6a**: $R_1$ = H, $R_2$ = OBn, X = H
**6b**: $R_1$ = H, $R_2$ = OBn, X =Br
**6c**: $R_1$ = H, $R_2$ = OBn, X = Me
**7a**: $R_1$ = OBn, $R_2$ = H, X = H
**7b**: $R_1$ = OBn, $R_2$ = H, X =Br
**7c**: $R_1$ = OBn, $R_2$ = H, X = Me

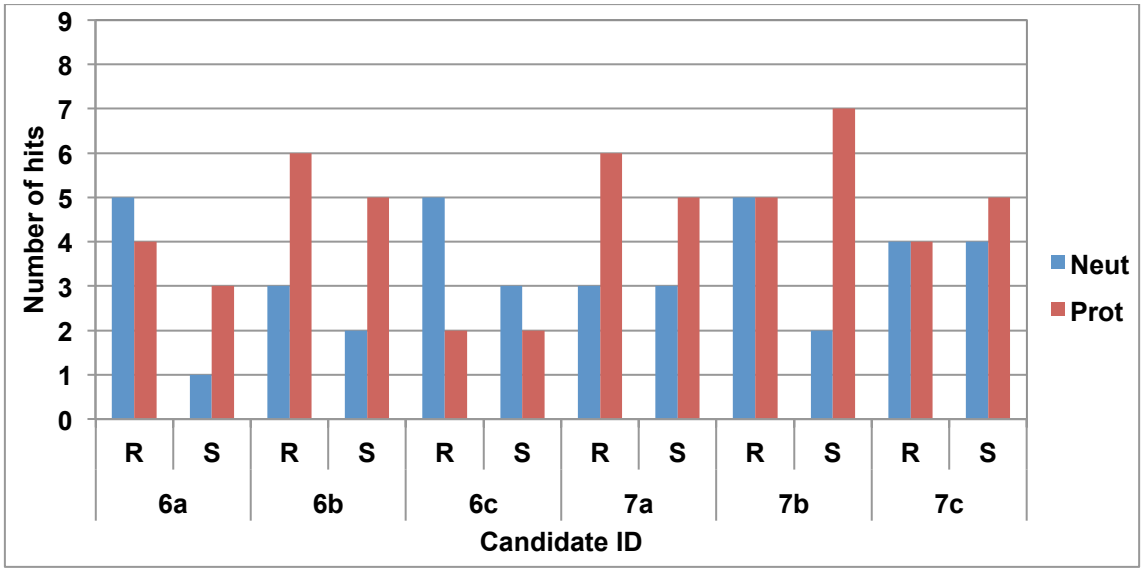


**Figure 12.** Global hit success that result from the docking to BACE-1 of indole derivatives, anilines (upper panel) and benzylamines (lower panel).

Moreover, for these latter compounds, the largest increase is observed for the hits containing a neutral ligand.

We have also studied the effect of the ligand protonation state on the number of hits. For the aniline as well as the benzylamine containing compounds (Figure 12), the number of hits increases (for the most part) when the amino group is protonated, rather than neutral.

**2.2 AChE ligand screening.**

The global hit rate resulting from the AChE docking based screening calculations for the indole derivatives that contain a substituted aniline or benzylamine in *ortho* or *meta* positions are depicted in Figure 13. Comparison of the effect of the substitution pattern in both aniline and benzylamine (shown in this figure) indicate that changing the substitution from *ortho* to *meta* increases the number of hits. As seen from Figure 13, the number of hits obtained and the consensus reached across the three scoring functions indicate that our indolebenzylamine-containing compounds fit well inside AChE spanning both the main site (CAS) and the peripheral one (PAS). Moreover, comparison of the aniline bearing compounds with the benzylamine ones indicate that the latter present a larger number of hits across all scoring functions, probably due to an increase in size of the ligands that allow it to span better both binding sites.

One interesting issue are the docking exit poses. As we mentioned above in our pharmacophore depiction for AChE, we seek to have dual inhibitors in which one of the end aromatic fragments is to be found at the CAS and the other end aromatic group positions itself in the PAS, both producing π stacking interactions with the aromatic residue clusters residing in both sites (see Figure 1). There are two possible pose orientations that fulfil this hit. In the first one the indole moiety is predicted to be found in the CAS while the terminal benzyloxi group is to be found at the PAS. In the second possible pose, we have the inverse option in which the indole fragment resides at the PAS. We have listed in Figure 13 both poses and have referred to them as 'CAS' and 'PAS' respectively. As seen from these plots the number of 'CAS' hits (indole docked into CAS) is larger than the one that places this fragment in the PAS (both for aniline and benzylamine containing compounds), a result that we will try to verify through X-ray crystallography. In Figure 14 we depict the most favoured pose obtained for compound **7a** with the Chemscore fitness function. Notice that the indole fits neatly in

the CAS, making π stacking interactions with residues W84 and F330, while the Bn group interacts with W279 and Y70 in the PAS.

Finally, our results (shown in Figure 13) indicate that there is scarcely a preference for one of the enatiomers, neither there is a clear proclivity for a neutral or charged state for the amino group.

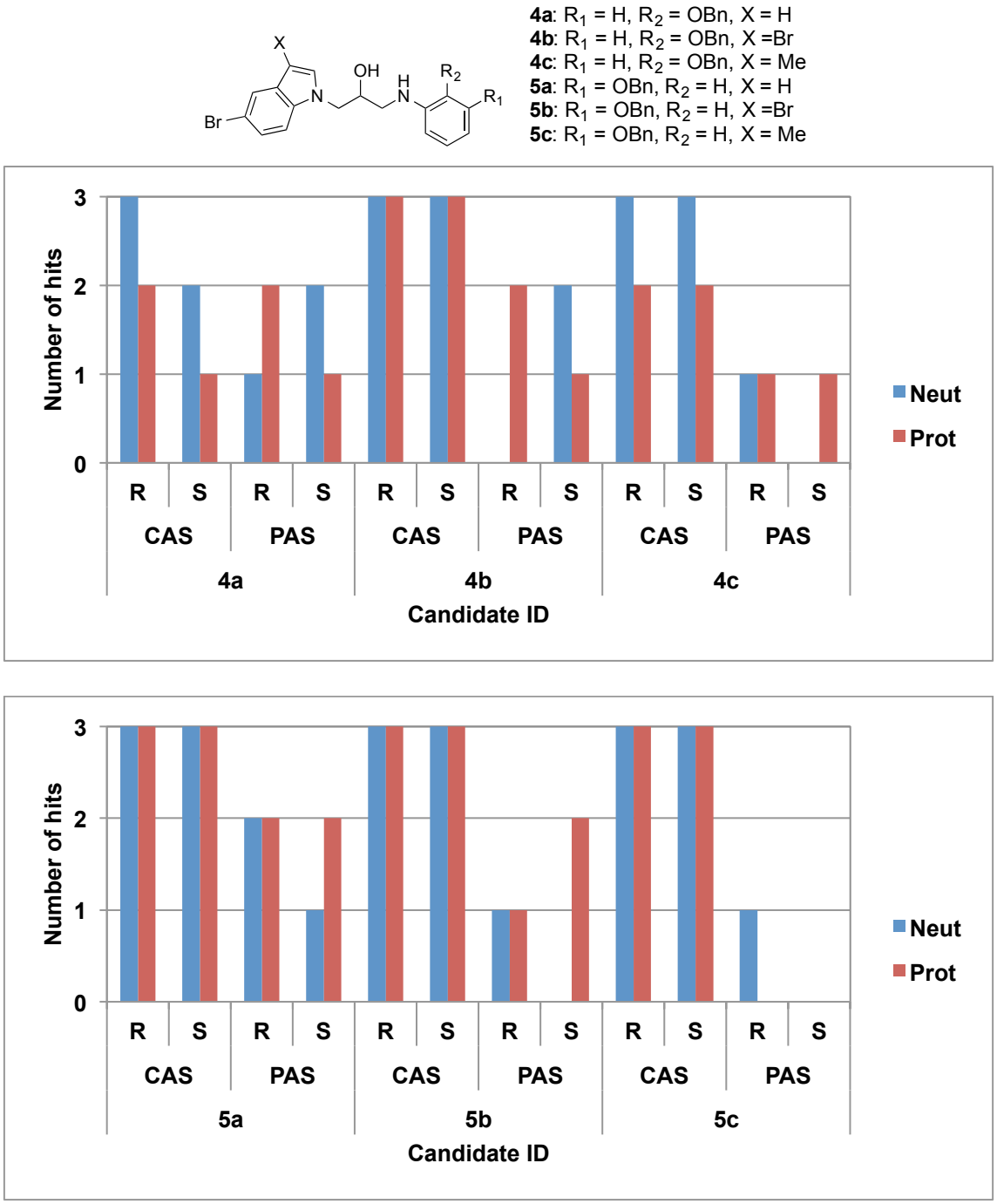


**Figure 13a.** Docking results of the indole bearing compounds with *ortho* (upper panel) and *meta* (lower panel) substituted anilines on AChE.

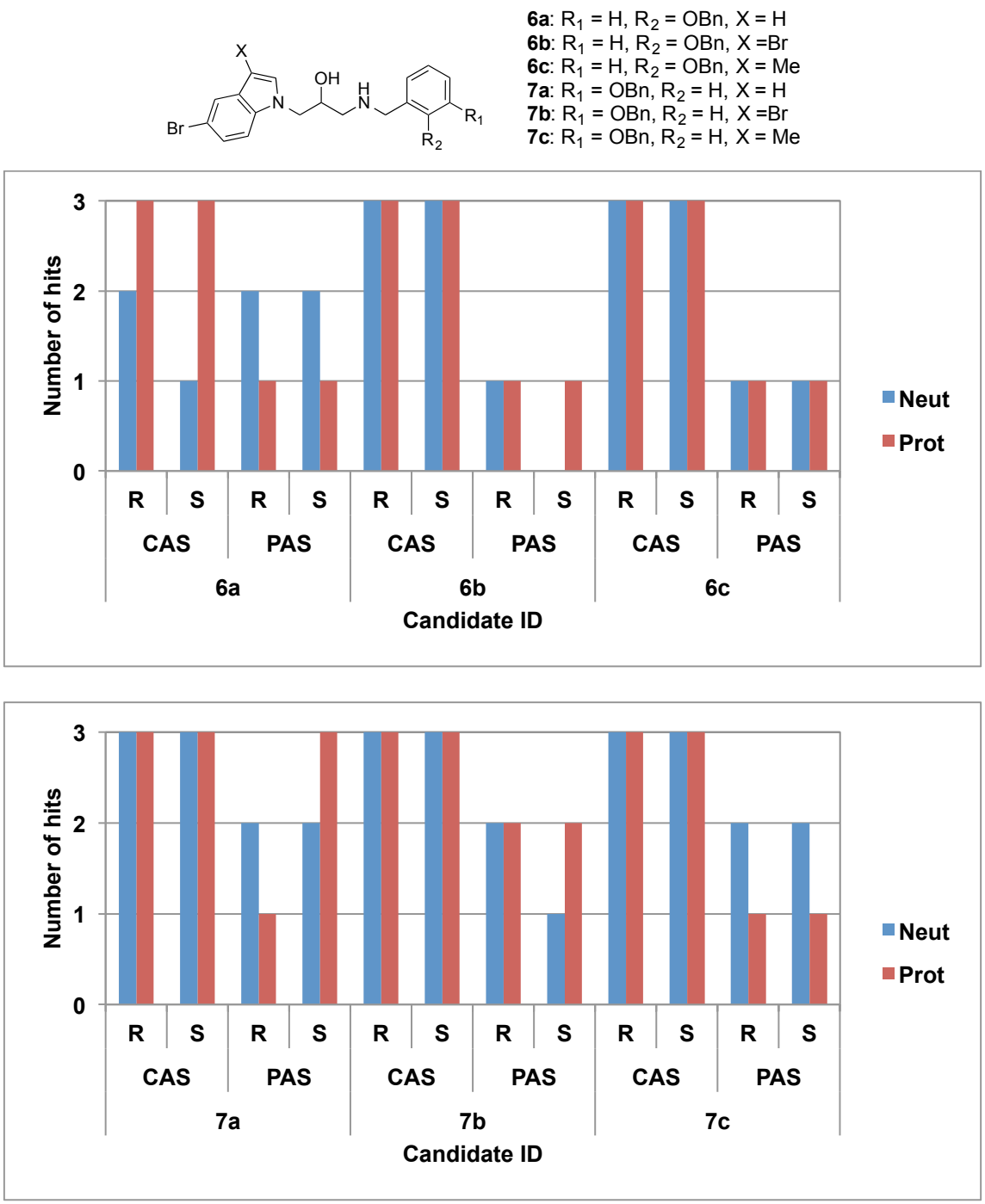


**Figure 13b.** Docking results for indole bearing compounds with *ortho* (upper panel) and *meta* (lower panel) substituted benzylamines on AChE.

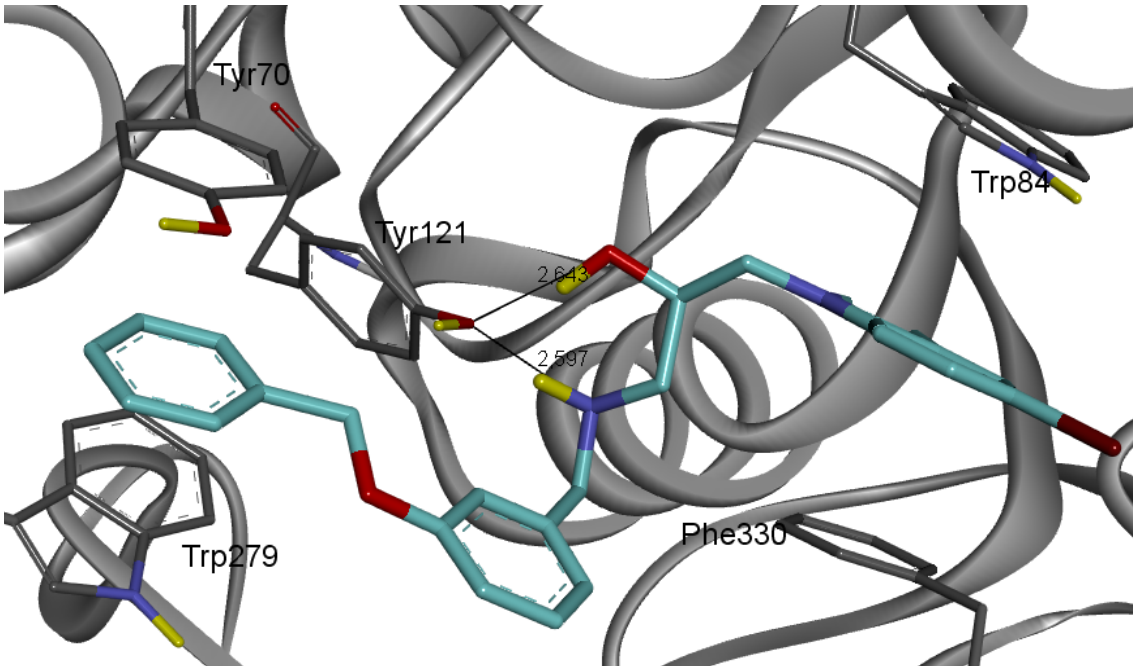


**Figure 14.** Pose for ligand **7a** in which the indole fragment interacts (through π stacking) with residues Trp 84 and Phe 330 in the CAS, while the treminal Bn group interacts with Tyr 70 and Trp 279 at the PAS site.

### 2.3. Inhibitor Aβ12-28 peptide interaction results.

We have performed the MD simulations on three of our indole candidates: one containing an aniline fragment (**4b**) and the other two containing a benzylamine moiety (**7b** and **7c**). The results indicate that percentage residency times around the peptide with 7.5 Å radii for these compounds are relatively high (88 ± 2.0, 96 ± 2.0 and 86 ± 1.30 respectively).

Figure 15 displays the ligands residency time around every residue of Aβ12-28. As seen from this figure, the ligands favour two binding spots (populated by aromatic residues), a result already observed for the carbazole containing compounds. The most frequented site is around the LVFFA segment, and the second one contains the two His residues at the start of the sequence. Another important feature is that these ligands present much higher residence times than the reference ligand, the 9,10-anthraquinone, a compound that has a 30% fibril formation inhibition at 100 μM concentration. Furthermore, comparison of the intra-peptide residue interaction when these two ligands are present (see Figure 16 and S4) with the residue contact when they are absent (see Figures 11 and S4) indicates that these compounds clearly interrupt the formation of the hairpin structures that are the hallmark of Aβ peptide aggregates, indicating that these ligands may inhibit amyloid aggregation. Finally, we predict that the benzylamine-containing

compounds (**7b** and **7c**) reduce the formation of turns (around the DVSG segment) more efficiently than the aniline based compound (**4b**).

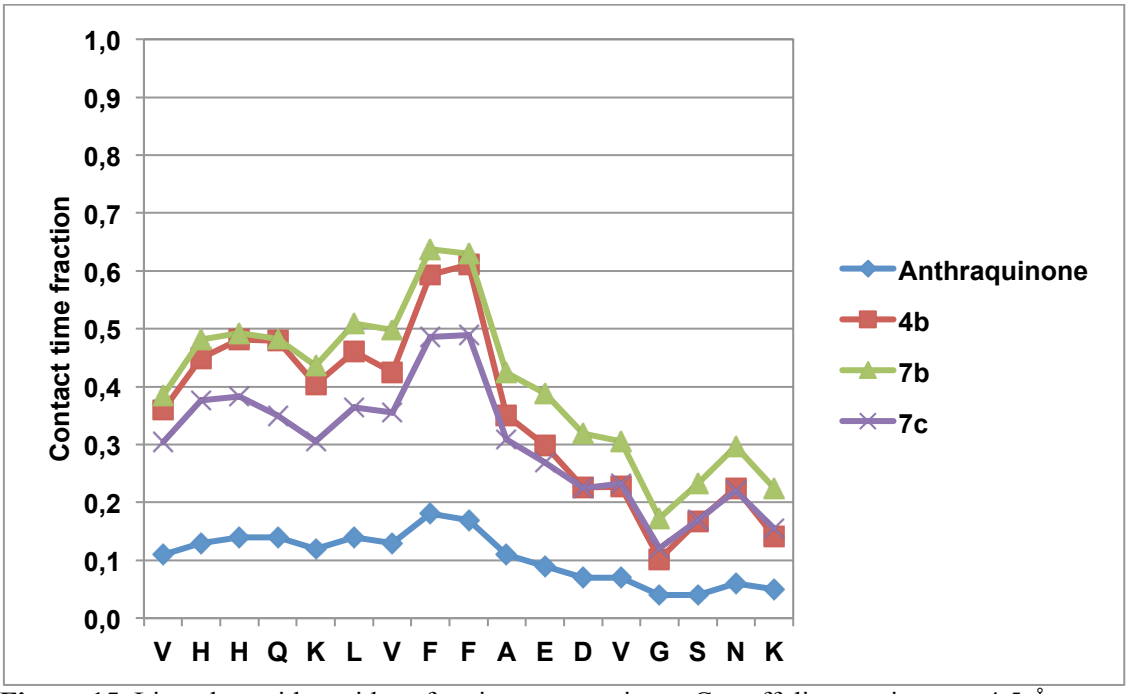


**Figure 15.** Ligand-peptide residues fraction contact times. Cut-off distance is set at 4.5 Å.

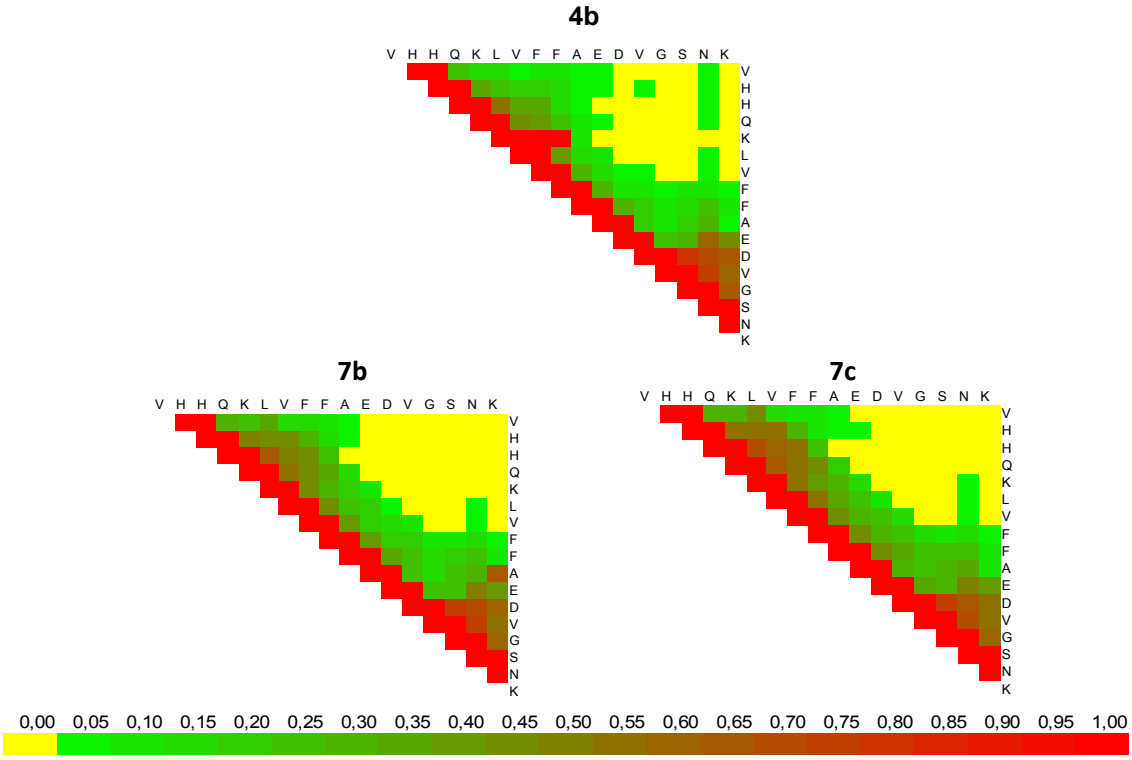


**Figure 16.** Residue-residue interaction contact map in the presence of the candidates **4b**, **7b** and **7c**. The colour scale shown above indicates the residence times.

**2.4. Synthesis and experimental assays for indole containing compounds**.

The indole derivatives whose structures contain either an aniline or a benzylamine fragment were obtained by the same synthetic route as the carbazole containing compounds indicated in Scheme 2, which includes the list of synthesized molecules.

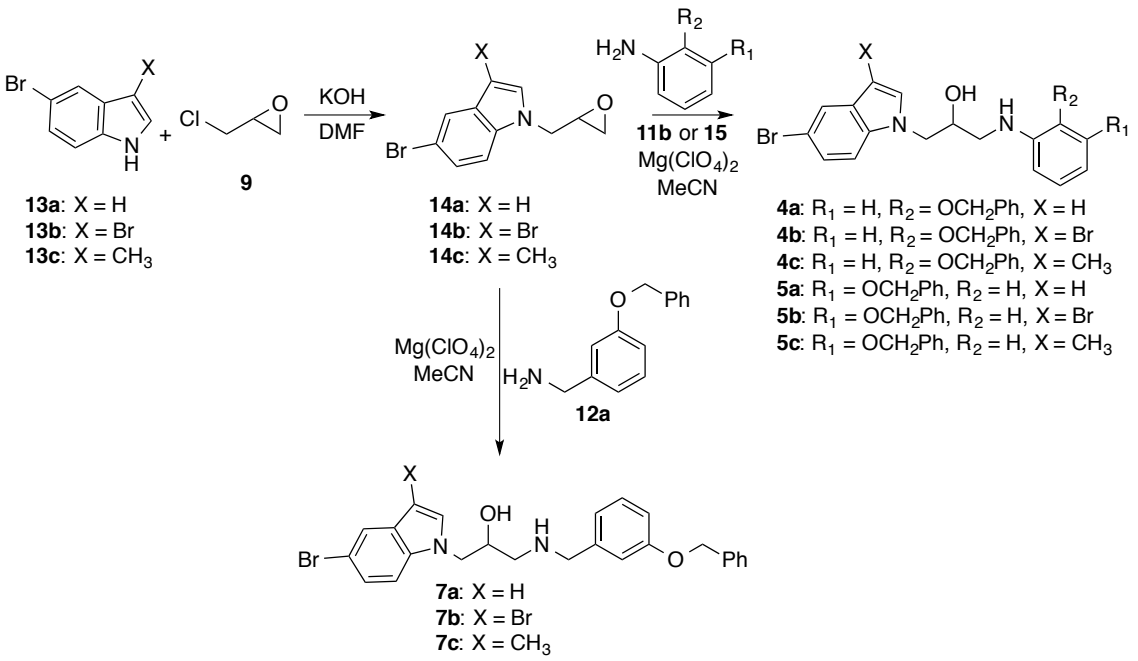


**Scheme 2.** Synthetic route and indole derivatives synthesized.

The results of the binding assays to BACE-1, AChE and BuChE for the selected compounds, together with the fibril inhibition assay are listed in Table 3. As seen from this table the *meta* substituted benzylamine compounds display altogether higher activity than the *ortho* substituted aniline ones for AChE, a result that validates the predictive power of our *in silico* protocol presented above. More importantly, the replacement of a carbazole by an indole moiety with a benzylamine substituted in *meta* has lead to candidates that bind **to all** chosen amyloid cascade targets, (BACE-1, amyloid aggregates and the peripheral site in AChE), as well as to AChE's main site and BuChE, implying also a positive cholinergic effect in AD. Hence, compounds like **7c** are truly multitarget compounds.

Finally, the results displayed in Tables 2 and 3 also afford us with important structural information for the binding poses of both carbazole and indole bearing compounds to the cholinergic targets. For instance compounds **7a, 7b** and **7c** bind even better to BuChE than to AChE. This result has structural implications, since these two enzymes

are highly homologous in the CAS, but BuChE replaces the targeted aromatic residues present in the PAS site of AChE by non-aromatic ones, precluding the formation of possible π stacking interactions in this enzyme.[36] Hence, the fact that there are ligands that bind to both cholinesterases may mean that they are able to diffuse to the CAS site in AChE and bind to it. This experimental results support the idea that our design has produced dual AChE inhibitors that bind both to the CAS and the PAS of this enzyme, a conclusion reached as well by the pose search in our docking based screening simulations (see Figures 13 and 14).

**Table 3.** Experimental results for indole based compounds.

| Candidate | *Ee*AChE | | hsBuChE | | Aβ(1-40) | | BACE-1 | |
|---|---|---|---|---|---|---|---|---|
| | %Inh.@ 10μM | $IC_{50}$(μM) | %Inh.@ 10μM | $IC_{50}$(μM) | %Inh.@ 100μM | $IC_{50}$(μM) | %Inh. @100μM | $IC_{50}$(μM) |
| **4a** | 44 ± 1 | -- | 17 ± 3 | -- | 43 ± 1 | -- | 5.7 ± 1.6 | -- |
| **4b** | 45 ± 2 | -- | 18 ± 3 | -- | 23 ± 2 | -- | 6.3 ± 1.4 | -- |
| **4c** | 44 ± 1 | -- | 19 ± 1 | -- | 43 ± 5 | -- | 16.4 ± 0.1 | -- |
| **5a** | -- | 8.5 ± 0.7 | 20 ± 2 | -- | 55 ± 3 | -- | 3.5 ± 2.4 | -- |
| **5b** | -- | 9.3 ± 0.6 | 24 ± 1 | -- | 22 ± 2 | -- | 1.8 ± 0.6 | -- |
| **5c** | -- | 12 ± 1 | 17 ± 1 | -- | 57 ± 2 | -- | 0.1 ± 0.1 | -- |
| **7a** | -- | 10.4 ± 0.1 | -- | 0.70 ± 0.02 | 57 ± 3 | -- | -- | 3.0 ± 1.4 |
| **7b** | -- | 9.1 ± 1.1 | -- | 0.29 ± 0.05 | 47 ± 2 | -- | -- | 2.5 ± 0.1 |
| **7c** | -- | 5.9 ± 1.0 | -- | 0.39 ± 0.03 | 78 ± 1 | 34 ± 2 | -- | 4.3 ±0 .8 |

## DISCUSSION & CONCLUSIONS

As mentioned in the introduction, the search for single leads for all chosen amyloid cascade targets represents a sizable challenge due to the substantial differences in their binding sites. To tackle this issue, we have proposed a two-step protocol. In the first step we have designed a pharmacophore, built around the knowledge obtained in our lab and others, that includes the interactions with the molecular targets that the candidates should fulfill. The resulting template allows for the automated screening of multiple candidates using programs like ZINCPharmer.[37] Our search for compounds in bibliographical data sets led us to a group of carbazole containing compounds with substituted aniline fragments, which has been previously identified as neuroprotective and neurogenerative compounds in mice.[8]

The second step of our method includes the evaluation and optimization of the initial set of compounds by a computer-assisted protocol that combines docking calculations for the enzyme targets (BACE-1 and AChE) with MD simulations for the in silico study of Abeta aggregation inhibition. The results of the docking calculations not only rely on obtaining the best scoring compounds, but more importantly on fulfilling the pattern of

interactions with the cardinal residues in our targets as shown in our pharmacophore scheme (see Figure 1). The MD simulations used for amyloid aggregation inhibition studied the time evolution of an amyloid peptide fragment in the presence and absence of our candidates, aimed at determining the strength of the binding to 'hot spot' peptide fragments, as well as understanding and evaluating the effect of the candidates on the peptide secondary structure.

Our computer-aided protocol was used with a twofold aim. Firstly, to investigate if the original compounds owed their known biologic activity to their binding to some the amyloid cascade targets, and secondly to search for analogues with an increased affinity for the largest possible group of amyloid cascade targets. The first round of calculations on our original compounds (that purportedly had neuroprotective and neurogenerative properties) displayed very few hits in BACE-1 (see Figure 5), but a number of hits in AChE. Our binding assays (Table 2) corroborated the outcome of our calculations, since the initial set of compounds displayed low affinities for BACE-1 (not surpassing the 33% BACE-1 inhibition at 1mM). Nevertheless, as predicted by our calculations these compounds presented μM affinity for AChE for those compounds that present the largest scoring function values in our docking calculations (see results for **1e** and **1f** in Figure 7). Perusal of the exit docking poses indicates that these compounds are able to span both AChE binding sites, a result that could explain their better affinity as compared to their congeners. Finally, some of the compounds in the initial set display a fibril formation inhibition slightly above that of the reference compound 9,10-anthraquinone.[35]

In order to improve the binding across the amyloid targets and especially for BACE-1, we proceeded to modify these compounds with the information afforded by two computer aided design cycles. The initial screening results for BACE-1 anticipated that most of the hits were obtained with the protonated amino group in the aniline (see Figure 5). In order to increase the probability that the amino group will actually be protonated we replaced the aniline moiety by a benzylamine fragment. The docking results predicted that the second generation compounds should improve their hit rates mainly for BACE-1. In order to test this outcome we synthesized and assayed two of the benzylamine containing compounds that showed promising results in the docking calculations (**3e** and **3f**). The binding assays indicated that the new candidates improved their binding affinities for BACE-1 by more than 3 orders of magnitude ($IC_{50}$ =3.1 μM). Interestingly enough, these compounds also showed affinity for BuChE. In healthy

brains, AChE hydrolyzes about 80% of acetylcholine while BuChE plays a secondary role. However, as AD progresses, the activity of AChE is greatly reduced in specific brain regions while BuChE activity increases, likely as a compensation for the AChE depletion.[38] Consequently, both enzymes are useful therapeutic targets for AD and our experimental results indicate that our compounds not only should affect the amyloid cascade at the core of the AD, but should have a positive cholinergic effect.[38]

The design of the third generation ligands was afforded by the inspection of the exiting poses of the carbazole containing compounds, which showed that there was some steric clashes between the carbazole moiety and some of the residues belonging either to BACE-1 and AChE (see Figures S1 and S2). In order to avoid close van der Waals overlaps we designed a new set of ligands in which the carbazole moiety was replaced by indole, a smaller fragment, while at the other end we kept the substituted aniline or benzylamine fragments. Even in the case of the aniline containing compounds, the replacement of a carbazole for an indole (see Figures 5 and 12) increases substantially the number of hits for BACE-1, especially when the ligand is neutral. Moreover, we predict that an additional hit enrichment could be obtained by replacing the aniline moiety by a benzylamine fragment substituted at *meta* rather than at *ortho* position (see Table S7 and Figure 12). Our docking calculations show that AChE has a very similar inhibitor preference as BACE-1, meaning that a consensus inhibitor design has been reached for both enzymes.

There has been a sizable effort in understanding the effect of ligands on the secondary structure of Abeta peptides by MD simulations, in order to get some insight on the inhibitory effect of these ligands.[28] For instance, Wang et al.[39] studied the time evolution of the Aβ peptide in the presence of polyphenolic xantones. The analysis of rather short MD simulations (in the nanosecond regime) indicated that the presence of these ligands seem to help retain the alpha helix secondary structure (from which these simulations start) and hence preclude amyloid aggregation. On the other hand the results of our calculations shed light on an open question that relates to the existence of an amyloidogenic core which serves as a template for amyloid oligomers and fibril formation, an issue that is relevant not only to AD but also to other pathologies (e.g., diabetes type 2 and Parkinson's) that are associated with the misfolding of polypeptides.[40] Hence, a possible paradigm for an Abeta aggregation route inhibition could rely on precluding the emergence of the template structure with a beta hairpin structure (around the DVGS motif) observed in various NMR experiments.[41]

Comparison of the results obtained from our MD simulations of an Aβ fragment (residues 12 to 28) in the presence and absence of our candidate compounds seem to indicate that the best aggregation inhibitors are able to modulate the secondary structure of the peptide, partially precluding the formation of a hairpin aggregation core. Perusal of Figures 10 and 15 indicate that the modulation of the secondary structure of the Abeta peptide is achieved by interaction of the ligand with the pairs of aromatic residues (predominantly Phe19-Phe20) present in the peptide segment studied. It was found that the hydrophobic interactions that involve these aromatic residues are vital for the genesis of the hairpin structure through the collapse of the hydrophobic stretch Leu17-Ala21.[41] The only other aromatic residues present in the full Abeta peptide are single aminoacids located in the segment comprised by the first eleven residues, that is known to lack any structure in peptide aggregates, and hence possibly do not have any role in inducing aggregation. Figure S3 displays a snapshot of the interaction between compound 7b and the Aβ12-28 peptide, as obtained from the MD simulation. As seen from this figure, there is a π stacking interaction between the aromatic core of the benzylamine fragment and one of the aromatic residues mentioned above.

We have calculated the variability, as given by the standard deviation (SD), of the crucial contacts between the segments DVGS and VHHQ in the MD trajectory (see Table S8 for some typical examples). The results indicate an increase in the SD values in the absence of a ligand, an outcome that indicates that the presence of our ligands seems to reduce the contact fluctuations, stabilizing secondary structures other than a turn.

There seems to be some relationship between the disruption of the aforementioned turn in our simulations and the result of the ThT assays. For instance, 9,10-anthraquinone, a compound that only inhibits 33% fibril formation, precludes to a much lesser extent the turn formation as compared to some of our best compounds like **7c**. Moreover, the indole/aniline derivative **4b** is much less effective in precluding the turn template as their benzylamine analogue **7b**, providing support for our MD simulation results. Nevertheless, we expect that this simple protocol based on MD simulations of a single Abeta peptide fragment may not be able to give a quantitative inhibition ranking, but rather would enable us to tell apart the binders from the inactive compounds. Presently, we are performing our MD simulations on a larger set of peptide-ligand complexes in order to validate the predictive capabilities of our protocol that could be useful in the design of Abeta aggregation inhibitors.

The results of the enzyme FRET assays for BACE-1, AChE and BuChE, as well as ThT fibril formation assays on indole based compounds with an aniline and *meta* substituted benzylamine derivatives fully support the outcome of our calculations, indicating that the latter set of compounds (**7a**, **7b** and **7c**) are by far the most superior candidates with highly improved ligand efficiency, and display a multitarget behaviour across the amyloid cascade and cholinergic pathways.

Besides affording robust predictions about the relative affinity of our candidate compounds, our computer assisted protocol has provided us with valuable structural predictions such as the flap opening in BACE-1 when bound to our inhibitors, or the orientation of the ligands in AChE, issues we are trying to verify by X-ray crystallography.

**ACKNOWLEDGMENTS**

Financial support from the Ministerio de Economia y Competitividad of Spain (Project CTQ2011-22436) and the Xunta de Galicia (2007/085 and 10CSA209063PR) is gratefully acknowledged. We would like to thank the Center for Supercomputing in Galicia (CESGA) for computer time and to Prof. Amedeo Caflisch for hosting one of us (J.L.D.) for a short term visit that allowed him to become familiar with the computer simulation protocols used in the study of amyloid aggregation.

**Supporting Information Available:** Additional data of docking to BACE-1 and AChE, as well as Aβ aggregation simulations, as described in the text. General materials and methods for syntheses and in vitro biological evaluation. This material is available free of charge via the Internet at http://pubs.acs.org.

**REFERENCES**

1. Mangialasche, F.; Solomon, A.; Winblad, B.; Mecocci, P.; Kivipelto, M. Alzheimer's disease: clinical trials and drug development. *Lancet Neurol.* **2010**, *9*, 702-716.

2. Walsh, D. M.; Selkoe, D. J. Deciphering the molecular basis of memory failure in Alzheimer's disease. *Neuron* **2004**, *44*, 181-193.

3. Selkoe, D. J. Preventing Alzheimer's disease. *Science* **2012**, *337*, 1488-1492.

4. Inestrosa, N. C.; Alvarez, A.; Pérez, C. A.; Moreno, R. D.; Vicente, M.; Linker, C.; Casanueva, O. I.; Soto, C.; Garrido, J. Acetylcholinesterase accelerates assembly of

amyloid-β-peptides into Alzheimer's fibrils: possible role of the peripheral site of the enzyme. *Neuron* **1996**, *16*, 881-891.

5. (a) Cavalli, A.; Bolognesi, M. L.; Capsoni, S.; Andrisano, V.; Bartolini, M.; Margotti, E.; Cattaneo, A.; Recanatini, M.; Melchiorre, C. A Small molecule targeting the multifactorial nature of Alzheimer's disease. *Angew. Chem. Int. Ed.* **2007**, *46*, 3689-3692. (b) Zhu, Y.; Xiao, K.; Ma, L.; Xiong, B.; Fu, Y.; Yu, H.; Wang, W.; Wang, X.; Hu, D.; Peng, H.; Li, J.; Gong, Q.; Chai, Q.; Tang, X.; Zhang, H.; Li, J.; Shen, J. Design, synthesis and biological evaluation of novel dual inhibitors of acetylcholinesterase and β-secretase. *Bioorg. Med. Chem.* **2009**, *17*, 1600-1613. (c) Fernández-Bachiller, M. I.; Pérez, C.; Monjas, L.; Rademann, J.; Rodríguez-Franco, M. I. New tacrine-4-oxo-4*H*-chromene hybrids as multifunctional agents for the treatment of Alzheimer's disease, with cholinergic, antioxidant, and β-amyloid-reducing properties. *J. Med. Chem.* **2012,** *55,* 1303-1317.

6. Viayna, E.; Gómez, T.; Galdeano, C.; Ramírez, L.; Ratia, M.; Badia, A.; Clos, M. V.; Verdaguer, E.; Junyent, F.; Camins, A.; Pallàs, M.; Bartolini, M.; Mancini, F.; Andrisano, V.; Arce, M. P.; Rodríguez-Franco, M. I.; Bidon-Chanal, A.; Luque, F. J.; Camps, P.; Muñoz-Torrero, D. Novel huprine derivatives with inhibitory activity toward β-amyloid aggregation and formation as disease-modifying anti-Alzheimer drug candidates. *Chem. Med. Chem.* **2010**, *5*, 1855-1870.

7. (a) Bolognesi, M. L.; Cavalli, A.; Valgimigli, L.; Bartolini, M.; Rosini, M.; Andrisano, V.; Recanatini, M.; Melchiorre, C. Multi-target-directed drug design strategy: From a dual binding site acetylcholinesterase inhibitor to a trifunctional compound against Alzheimer's disease. *J. Med. Chem.* **2007,** *50,* 6446-6449. (b) Bolognesi, M. L.; Bartolini, M.; Tarozzi, A.; Morroni, F.; Lizzi, F.; Milelli, A.; Minarini, A.; Rosini, M.; Hrelia, P.; Andrisano, V.; Melchiorre, C. Multitargeted drugs discovery: Balancing anti-amyloid and anticholinesterase capacity in a single chemical entity. *Bioorg. Med. Chem.* **2011**, *21*, 2655-2658. (c) Li, R.-S.; Wang, X.-B.; Hu, X.-J.; Kong, L.-Y. Design, synthesis and evaluation of flavonoid derivatives as potential multifunctional acetylcholinesterase inhibitors against Alzheimer's disease. *Bioorg. Med. Chem. Lett.* **2013**, *23*, 2636-2641.

8. McMillan, K. S.; Naidoo, J.; Liang, J.; Melito, L.; Williams, N. S.; Morlock, L.; Huntington, P. J.; Estill, S. J.; Longgood, J.; Becker, G. L.; McKnight, S. L.; Pieper, A. A.; De Brabander, J. K.; Ready, J. M. Development of proneurogenic, neuroprotective small molecules. *J. Am. Chem. Soc.* **2011**, *133*, 1428-1437.

9. Yuan, J.; Venkatraman, S.; Zheng, Y.; McKeever, B. M.; Dillard, L. W.; Sing, S. B. Structure-based design of *β*-site APP cleaving enzyme 1 (BACE1) inhibitors for the treatment of Alzheimer's disease. *J. Med. Chem.* **2013**, *56*, 4156–4180.

10. Domínguez, J. L.; Christopeit, T.; Villaverde, M. C.; Gossas, T.; Otero, J. M.; Nyström, S.; Baraznenok, V.; Lindström, E.; Danielson, U. H.; Sussman, F. Effect of the protonation state of the titratable residues on the inhibitor affinity to BACE-1. *Biochemistry* **2010**, *49*, 7255-7263.

11. Sussman, F.; Villaverde, M. C.; Domínguez, J. L.; Danielson, U. H. On the active site protonation state in aspartic proteases: implications for drug design. *Curr. Pharm. Design* **2013**, *19*, 4257-4275.

12. Dvir, H.; Silman, I.; Harel, M.; Rosenberry, T. L.; Sussman, J. L. Acetylcholinesterase: from 3D structure to function. *Chem.-Biol. Interact.* **2010**, *187*, 10-22.

13. Hopkins, C. R. ACS chemical neuroscience molecule spotlight on dimebon. *ACS Chem. Neurosci.* **2010**, *1*, 587-588.

14. Yang, W.; Wong, Y.; Ng, O. T. W.; Bai, L.-P.; Kwong, D. W. J.; Ke, Y.; Jiang, Z.-H.; Li, H.-W.; Yung, K. K. L.; Wong, M. S. Inhibition of beta-amyloid peptide aggregation by multifunctional carbazole-based fluorophores. *Angew. Chem.* **2012**, *124*, 1840-1846.

15. GOLD, version 5.1, Cambridge Crystallographic Data Centre, Cambridge, UK.

16. Jones, G.; Willett, P.; Glen, R.C. Molecular recognition of receptor sites using a genetic algorithm with a description of desolvation. *J. Mol. Biol.* **1995**, 245, 43-53.

17. Jones, G.; Willett, P.; Glen, R. C.; Leach, A. R.; Taylor, R. Development and validation of a genetic algorithm for flexible docking. *J. Mol. Biol.* **1997**, *267*, 727-748.

18. Baxter, C. A.; Murray, C. W.; Clark, D. E.; Westhead, D. R.; Eldridge, M. D. Flexible docking using tabu search and an empirical estimate of binding affinity. *Proteins* **1998**, *33*, 367-382.

19. Eldridge, M. D.; Murray, C. W.; Auton, T. R.; Paolini, G. V.; Mee, R. P. Empirical scoring functions: I. The development of a fast empirical scoring function to estimate the binding affinity of ligands in receptor complexes. *J. Comput. Aided Mol. Des.* **1997**, *11*, 425-445.

20. Verdonk, M. L.; Cole, J. C.; Hartshorn, M. J.; Murray, C. W.; Taylor, R. D. Improved protein-ligand docking using GOLD. *Proteins* **2003**, *52*, 609-623.

21. Korb, O.; Stützle, T.; Exner, T. E. Empirical scoring functions for advanced protein-ligand docking with PLANTS. *J. Chem. Inf. Model.* **2009**, *49*, 84-96.

22. Hong, L.; Koelsch, G.; Lin, X.; Wu, S.; Terzyan, S.; Ghosh, A. K.; Zhang, X. C.; Tang, J. Structure of the protease domain of memapsin 2 (β-secretase) complexed with inhibitor. *Science* **2000**, *290*, 150-153.

23. Wang, Y.-S.; Strickland, C.; Voigt, J. H.; Kennedy, M. E.; Beyer, B. M.; Senior, M. M.; Smith, E. M.; Nechuta, T. L.; Madison, V. S.; Czarniecki, M.; McKittrick, B. A.; Stamford, A. W.; Parker, E. M.; Hunter, J. C.; Greenlee, W. J.; Wyss, D. F. Application of fragment-based NMR screening, X-ray crystallography, structure-based design, and focused chemical library design to identify novel $\mu$M leads for the development of nM BACE-1 ($\beta$-site APP cleaving enzyme 1) inhibitors. *J. Med. Chem.* **2010**, *53*, 942-950.

24. Patel, S.; Vuillard, L.; Cleasby, A.; Murray, C. W.; Yon, J. Apo and inhibitor complex structures of BACE (β-secretase). *J. Mol. Biol.* **2004**, *343*, 407-416.

25. Discovery Studio, versions 2.1 and 2.5. Accelrys Inc., San Diego, CA

26. Rydberg, E. H.; Brumshtein, B.; Greenblatt, H. M.; Wong, D. M.; Shaya, D.; Williams, L. D.; Carlier, P. R.; Pang, Y.-P.; Silman, I.; Sussman, J. L. Complexes of alkylene-linked tacrine dimers with *Torpedo californica* acetylcholinesterase: binding of bis(5)-tacrine produces a dramatic rearrangement in the active-site gorge. *J. Med. Chem.* **2006**, *49*, 5491-5500.

27. (a) Convertino, M.; Vitalis, A.; Caflisch, A. Disordered binding of small molecules to A$\beta$(12-28). *J. Biol. Chem.* **2011**, *286*, 41578-41588. (b) Scherzer-Attali, R.; Pellarin, R.; Convertino, M.; Frydman-Marom, A.; Egoz-Matia, N.; Peled, S.; Levy-Sakin, M.; Shalev, D. E.; Caflisch, A.; Gazit, E.; Segal, D. Complete phenotypic recovery of an Alzheimer's disease model by a quinone-tryptophan hybrid aggregation inhibitor. PLoS ONE, **2010**, *5*, e11101. (c) Scherzer-Attali, R.; Convertino, M.; Pellarin, R.; Gazit, E.; Segal, D.; Caflisch, A. Methylations of tryptophan-modified naphthoquinone affect its inhibitory potential toward A$\beta$ aggregation. *J. Phys. Chem. B* **2013**, *117*, 1780-1789.

28. Lemkul, J. A.; Bevan, D. R. The role of molecular simulations in the development of inhibitors of amyloid $\beta$-peptide aggregation for the treatment of Alzheimer's disease. *ACS Chem. Neurosci.* **2012**, *3*, 845-856.

29. Lührs, T.; Ritter, C.; Adrian, M., Riek-Loher, D.; Bohrmann, B.; Döbeli, H.; Schubert, D.; Riek, R. 3D structure of Alzheimer's amyloid-$\beta$(1-42) fibrils. *Proc. Natl. Acad. Sci. U.S.A.* **2005**, *102*, 17342-17347.

30. Brooks, B. R.; Bruccoleri, R. E.; Olafson, B. D.; States, D. J.; Swaminathan, S.; Karplus, M. CHARMM: a program for macromolecular energy, minimization, and dynamics calculations. *J. Comput. Chem.* **1983**, *4*, 187-217.

31. Haberthür, U.; Caflisch, A. FACTS: fast analytical continuum treatment of solvation. *J. Comput. Chem.* **2008**, *29*, 701-715.

32. Domínguez, J. L.; Villaverde, M. C.; Sussman, F. Effect of pH and ligand charge state on BACE-1 fragment docking performance. *J. Comput Aided Mol. Des.* **2013**, *27*, 403-417.

33. Asso, V.; Ghilardi, E.; Bertini, S.; Digiacomo, M.; Granchi, C.; Minutolo, F.; Rapposelli, S.; Bortolato, A.; Moro, S.; Macchia, M. $\alpha$-Naphthylaminopropan-2-ol derivatives as BACE1 inhibitors. *Chem. Med. Chem.* **2008**, *3*, 1530-1534.

34. Paleo, M. R.; Aurrecoechea, N.; Jung, K.-Y.; Rapoport, H. Formal enantiospecific synthesis of (+)-FR900482. *J. Org. Chem.* **2003**, *68*, 130-138.

35. Convertino, M.; Pellarin, R.; Catto, M.; Carotti, A.; Caflisch, A. 9,10-Anthraquinone hinders β-aggregation: How does a small molecule interfere with Aβ-peptide amyloid fibrillation? *Protein Sci.* **2009**, *18*, 792-800.

36. Nicolet, Y.; Lockridge, O.; Masson, P.; Fontecilla-Camps, J. C.; Nachon, F. Crystal structure of human butyrylcholinesterase and of its complexes with substrate and products. *J. Biol. Chem.* **2003**, *278*, 41141-41147.

37. Koes, D. R.; Camacho, C. J. ZINCPharmer: pharmacophore search of the ZINC database. *Nucleic Acids Res.* **2012**, *40*, W409-W414.

38. Li, S.-Y.; Jiang, N.; Xie, S.-S.; Wang, K. D. G.; Wang, X.-B-; Kong, L.-Y. Design, synthesis and evaluation of novel tacrine-rhein hybrids as multifunctional agents for the treatment of Alzheimer's disease. *Org. Biomol. Chem*. **2014**, *12*, 801-814.

39. Wang, Y.; Xia, Z.; Xu, J.-R.; Wang, Y.-X.; Hou, L.-N.; Qiu, Y.; Chen, H.-Z. α-Mangostin, a polyphenolic xanthone derivative from mangosteen, attenuates β-amyloid oligomers-induced neurotoxicity by inhibiting amyloid aggregation. *Neuropharmacology* **2012**, *62*, 871-881.

40. Buchanan, L. E.; Dunkelberger, E. B.; Tran, H. Q.; Cheng, P.-N.; Chiu, C.-C.; Cao, P.; Raleigh, D. P.; de Pablo, J. J.; Nowick, J. S.; Zanni, M. T. Mechanism of IAPP amyloid fibril formation involves an intermediate with a transient β-sheet. *Proc. Natl. Acad. Sci. U.S.A.* **2013**, *110*, 19285-19290.

41. Ahmed, M.; Davis, J.; Aucoin, D.; Sato, T.; Ahuja, S.; Aimoto, S.; Elliot, J. I.; Van Nostrand, W. E.; Smith, S. O. Structural conversion of neurotoxic amyloid-$\beta_{1-42}$ oligomers to fibrils. *Nat. Struct. Mol. Biol*. **2010**, *17*, 561-567.

**TOC graphic:**